Abdominal Radiology (2023) 48:1479–1504
https://doi.org/10.1007/s00261-023-03830-3

REVIEW

Beyond the abdominal and pelvic cavity: abdominal wall and spinal "Aunt Minnies"

Ryan Thompson[1,2,5] · Noushin Vahdat[1,2] · Wael Alshehri[1,3] · Lejla Aganovic[1,2] · Saif Baig[1] · Sara Mirza[1] · Holly Cassidy[4] · Fiona Hughes[1,2]

Received: 29 September 2022 / Revised: 19 January 2023 / Accepted: 23 January 2023 / Published online: 15 February 2023

Abstract

Abdominal wall and spinal soft tissue findings are frequently encountered on CT or MR imaging of the abdomen and pelvis. Many of these entities have specific imaging findings, for which a definitive diagnosis can be made without the need for further work up. These abdominal wall and spinal findings may be diagnostically challenging for sub-specialized abdominal radiologists who are unfamiliar with their appearance and appropriate management. This review article describes and illustrates pathognomonic or characteristic abdominal wall and spinal pathologies, which reside outside the abdominopelvic cavity. The cases selected all have findings that allow a confident diagnosis without further imaging or intervention. The cases presented include myonecrosis, intramuscular abscess, myositis, iliopsoas bursitis, Morel-Lavallée lesion, hydrocele of canal of Nuck, Klippel Trenaunay Weber syndrome, neurofibroma with target sign, perineural cysts, filum terminale lipoma, calvarial bone flap, transverse rectus abdominis muscle (TRAM) flap, liposuction, and hidradenitis suppurativa, among others. Although not all-encompassing, this paper will help abdominal radiologists to accurately diagnose a variety of abdominal and pelvic extra-cavitary soft tissue pathologies by identifying key radiologic findings.

✉ Ryan Thompson
r2thompson@health.ucsd.edu

1 University of California San Diego, San Diego, CA, USA

2 VA Healthcare System, San Diego, CA, USA

3 King Khalid University, Abha, Saudi Arabia

4 Torrey Pines High School, San Diego, CA, USA

5 Department of Radiology, UC San Diego Health, 200 W Arbor Drive, San Diego, CA 92103-8756, USA

Graphical abstract

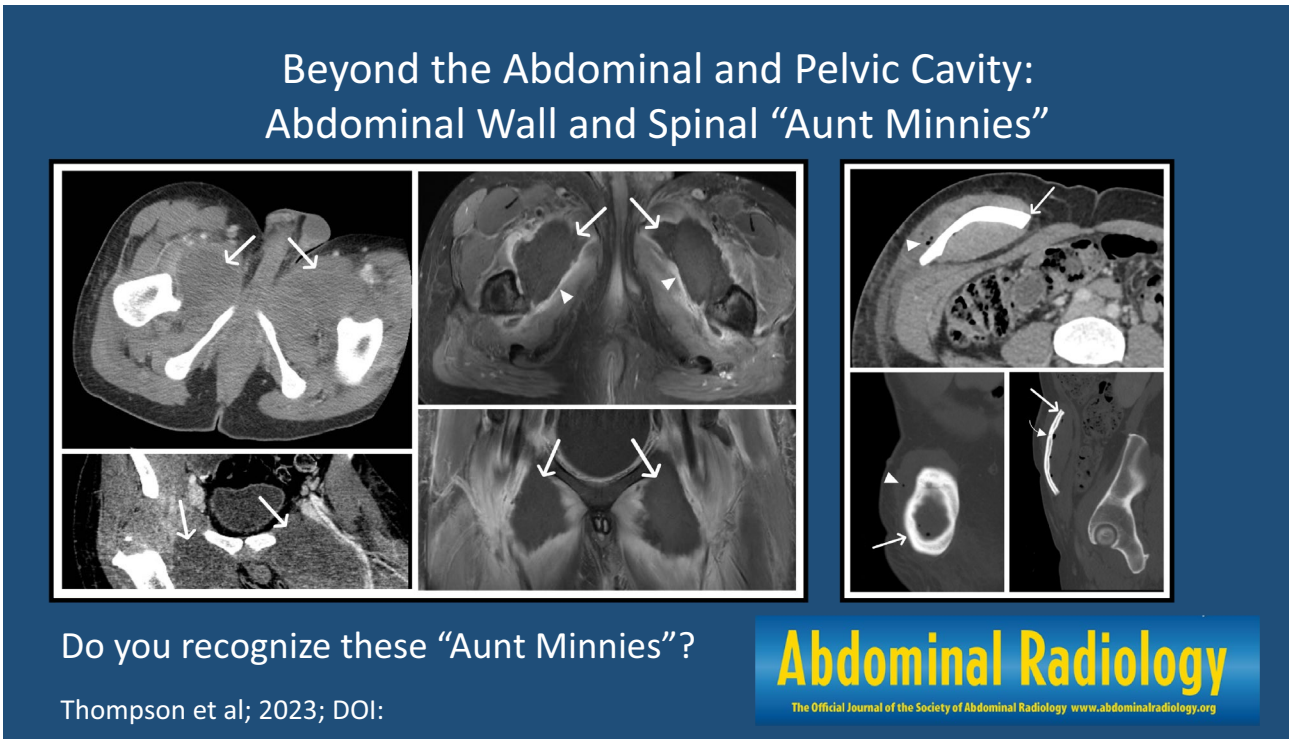

Keywords Neurofibromatosis · Klippel Trenaunay Weber syndrome · Myonecrosis · Liposuction · Tarlov cysts · Hidradenitis suppurativa

Introduction

Imaging of the abdomen and pelvis frequently reveals incidental skin, subcutaneous, muscular, and neurological abnormalities residing outside the abdominopelvic cavity. This can pose a diagnostic dilemma for the abdominal radiologist who may not be familiar with the appearance, differential considerations, and appropriate workup. There have been multiple recent articles to address this [1–3]; however, most articles focused primarily on osseous incidental findings in the abdomen and pelvis with little discussion of soft tissue findings. A recent paper [4] reviewed the imaging findings of many abdominal wall masses, but did not include spinal soft tissue lesions.

This article intends to help the abdominal radiologist become more comfortable in recognizing and diagnosing soft tissue entities occurring outside the abdominopelvic cavity, which may be encountered in abdominal and pelvic imaging. This is not meant to be a comprehensive essay, but rather a review of pathognomonic or characteristic entities, so-called "Aunt Minnies," seen on abdominal CT and MRI in our practice. Cases were selected where abdominal radiologists could have arrived at a definitive diagnosis but failed to recognize key findings which initiated unnecessary additional imaging or tissue sampling. For example, the pectineus muscle myonecrosis case (Fig. 1) was initially misdiagnosed as intramuscular abscess and the ossified iliac subperiosteal hematoma case (Fig. 25) was initially misdiagnosed as an indeterminate bone lesion requiring further workup.

The term "Aunt Minnie" is shorthand for a classic, often, radiological appearance of a pathology. The term was originally used by Dr. Neuhauser (1908–1987), Chief of Radiology at Boston Children's Hospital [5]. The Aunt Minnie approach was that you would easily recognize your Aunt Minnie in a crowd, just by gestalt. The original meaning has been slightly expanded so that an "Aunt

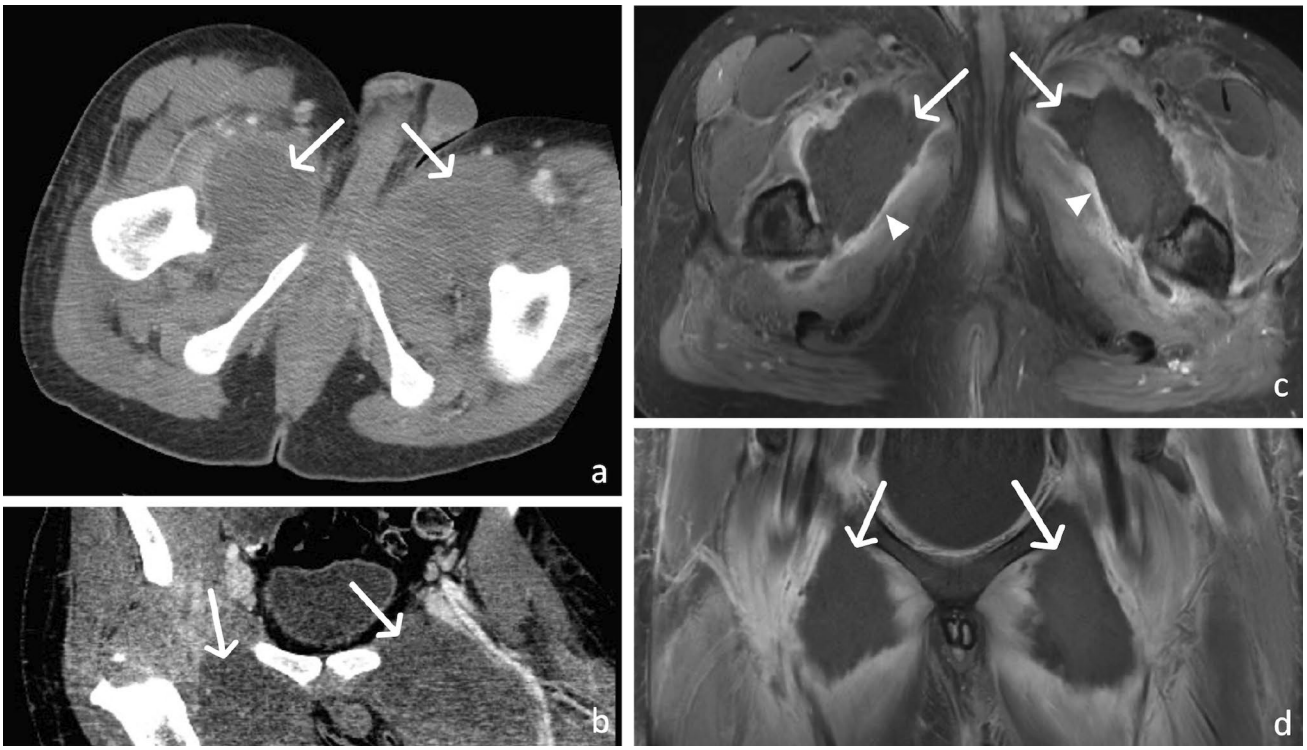

Fig. 1 43-year-old male with bilateral pectineal muscle myonecrosis. Axial (**a**) and coronal (**b**) CT images of the abdomen and pelvis demonstrate ill-defined muscle enlargement and decreased attenuation of bilateral anteromedial compartments of the upper thighs (arrows). Axial (**c**) and coronal (**d**) T1W fat-saturated post-contrast MR images demonstrate bilateral peripheral enhancement (arrowheads) of the pectineus muscles surrounding central non-enhancing (arrows) muscle fibers representing myonecrosis

Minnie" now means any classic constellation of findings which should raise a specific diagnosis [6, 7].

In this review we will characterize imaging findings of various abdominal wall and spinal "Aunt Minnies" and will highlight salient teaching pearls to guide the abdominal radiologist reach the most accurate diagnosis (Table 1).

Muscular lesions

Myonecrosis

Myonecrosis, also known as muscle infarction, refers to necrosis of muscle fibers. It is most often a complication of late-stage diabetes; however, it is also associated with rhabdomyolysis, severe ischemia, compartment syndrome, crush injury, sickle-cell crisis, and intra-arterial chemotherapy. Often the radiologist will first suspect this condition based on imaging characteristics [8]. The thigh muscles are most commonly affected, and the patient typically presents with pain and low-grade fever without leukocytosis. Imaging may show peripheral enhancement around non-enhancing areas of muscle, representing necrosis on postcontrast images (Figs. 1 and 2). Typically, there is diffuse increased muscular signal, although less than fluid signal, on T2-weighted (T2W) sequences, representing edema [9]. Although not always seen, foci of enhancement within the affected muscle may be present, termed the "stipple sign [9]" (Fig. 3). This should not be confused for intramuscular abscess, especially in the absence of leukocytosis or other infectious symptoms. Although an intramuscular abscess will also show rim enhancement, it should have fluid signal centrally [9] and will be more focal (Fig. 4) as compared to myonecrosis which typically conforms to the shape of the muscle and the abnormality runs parallel to the muscle fibers.

Table 1 Teaching points for abdominal wall and spinal "Aunt Minnie's" in abdomen and pelvis CT and MR

Consider myonecrosis, rather than intramuscular abscess, when presented with an intramuscular lesion which aligns with muscle fibers, especially when bilateral, symmetric, and in the absence of leukocytosis
Look for central fluid signal to help confidently differentiate an abscess from myonecrosis, especially on MRI
Myositis will show diffuse enhancement of the affected muscle while myonecrosis will show hypoenhancement
Iliopsoas bursitis will be seen in the expected location of the iliopsoas bursa and often communicates with the hip joint, differentiating this from abscess
Abdominal muscle strains are a common cause for abdominal pain in young patients. Look for hypoattenuating abdominal musculature, sometimes best appreciated on coronal reformats
The target sign suggests a peripheral nerve sheath tumor. The interval loss of a target sign is suggestive of malignant transformation
Perineural (Tarlov's) cysts will not enhance, which helps distinguish from peripheral nerve sheath tumors
Fat attenuating lesion in the filum terminale represents a filum terminale lipoma, a common incidental finding on CT and MRI, which requires no follow-up in an asymptomatic patient. However, it can be associated with the clinical entity of tethered cord syndrome. Additional signs to evaluate for include a low-lying conus or filum thickening on MRI
Superficial cystic lesions, especially about the hips, may represent a post-traumatic Morel-Lavallée lesion. It is important to differentiate this from a hematoma, as the clinical management may differ significantly
Soft tissue thickening of the superficial and deep subcutaneous tissues with locules of macroscopic fat may represent a sclerosing lipogranulomatous reaction related to injection of exogenous oils, free-silicone, or implant rupture
A characteristic finding of recent liposuction is a thick linear band running parallel to the skin with thinner perpendicular bands representing the cannula insertion tracks
Transverse rectus abdominis (TRAM) flap reconstruction is commonly seen after mastectomy and is characterized by the presence of an atrophied muscle anterior to the chest wall, the absence of normal glandular breast tissue, the absence of a normal rectus abdominis muscle, and the presence of surgical clips
After decompressive craniectomy, the removed calvarial bone fragments may be stored in vivo in the subcutaneous tissue of the patient. Complications include infection and bone resorption
Hidradenitis suppurativa is a chronic inflammatory skin disease involving the folliculopilosebaceous units in apocrine sweat gland rich areas of the body, typically affecting the genitofemoral area and axillae with severe typically bilateral skin thickening, edema of the subcutaneous tissues, and formation of multiple small subcutaneous abscesses, sinuses and fistulae
A cystic structure in the inguinal canal of female patients extending toward the labia may represent a Canal of Nuck hydrocele. Complications include herniation of bowel or pelvic organs, incarceration of bowel, and ovarian torsion within the canal
Expansile iliac osseous lesions in patients with a history of trauma may represent a chronic ossified subperiosteal hematoma. Look for the "ghost native cortex" sign to distinguish from fibrous dysplasia. This should not be confused for a lytic osseous lesion and represents a "do not touch" entity

Myositis

In contradistinction to myonecrosis, myositis refers to inflammation of the muscle fibers. Types of myositis include infectious, inflammatory, drug-related, traumatic, and iatrogenic [10]. In the acute phase, this will classically present as edema with high T2W and STIR signal with diffuse enhancement (Fig. 5), distinguishing it from myonecrosis. In the chronic form, this may be associated with an increased T1-weighted (T1W) signal, representing muscular atrophy and fat deposition.

Iliopsoas bursitis

Although not truly a muscular lesion, it is important to distinguish iliopsoas bursitis from other rim-enhancing lesions described here, such as myonecrosis and abscess. The iliopsoas bursa is a large synovial bursa located between the musculotendinous portion of the iliopsoas muscle and the anterior capsule of the hip [11]. Iliopsoas bursitis refers to inflammation of the bursa and is characterized by distension of the bursa [11]. Imaging findings include a well-defined, thin-walled, cystic mass with a communication to the hip

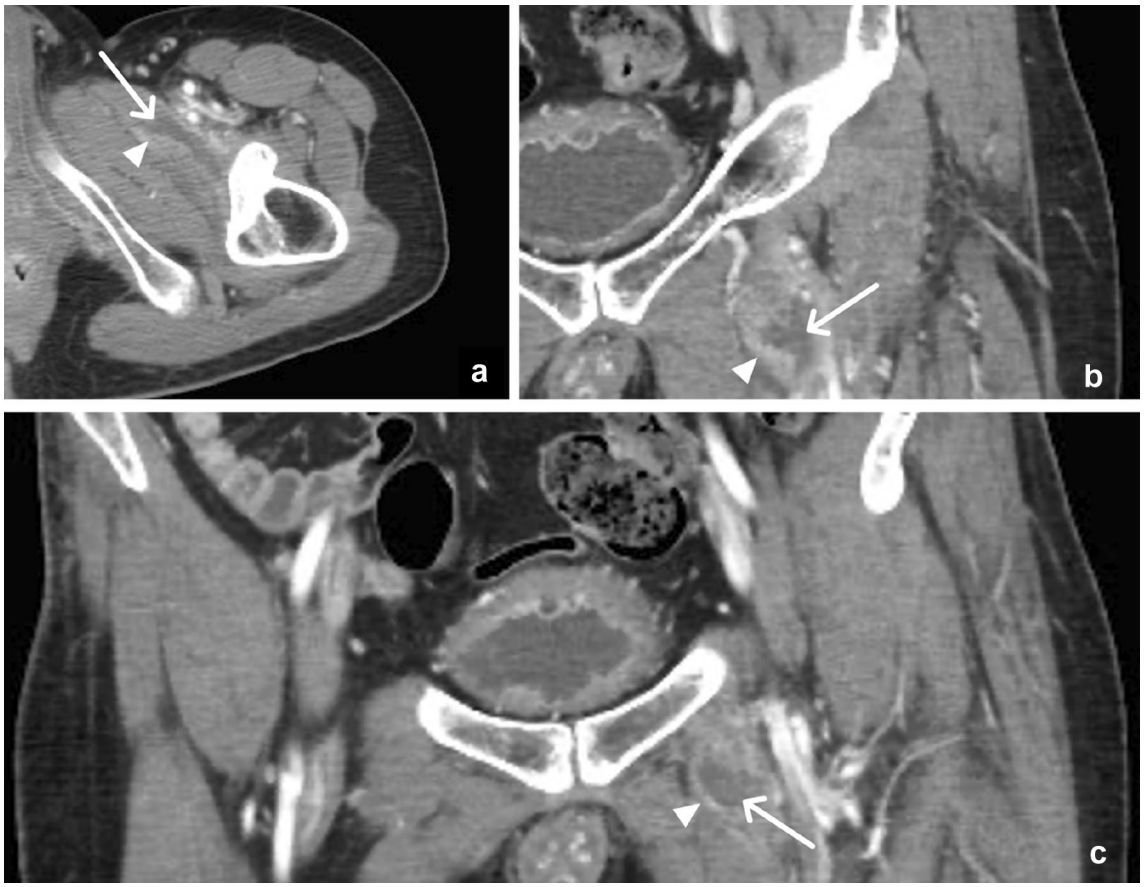

Fig. 2 45-year-old male with left pectineal muscle myonecrosis. Axial (**a**) and coronal (**b**, **c**) contrast-enhanced CT images demonstrate peripheral enhancement (arrowheads) surrounding a centrally hypoattenuating (arrows) left pectineus muscle

joint which may have peripheral contrast enhancement [12] (Fig. 6).

Rectus abdominis muscle strain

The abdominal wall musculature can undergo tear and strain, either as a result of blunt trauma or abrupt movement such as twisting or a rapid change in position. Rectus abdominis muscle strains are common and debilitating injuries among competitive young athletes, and usually present as abdominal pain. On CT, irregular contour and linear low attenuation of the rectus abdominis muscle is usually observed. MRI images often demonstrate hyperintense signal on fluid-sensitive sequences with intrinsic high signal on (T1W) sequences due to the presence of blood products (Fig. 7) [13, 14].

Nerve related lesions

Schwannoma and neurofibroma

Given the large number of exiting spinal nerves in the abdomen and pelvis, peripheral nerve-sheath tumors are commonly encountered. Schwannomas and neurofibromas can be found anywhere along a peripheral nerve, and these two histologically distinct tumors share many imaging features. These tumors are usually less than 5 cm in diameter and on MRI have slightly greater signal than muscle on T1W images and exhibit high signal on T2W images. The "target sign," where the center of the tumor is low in signal on T2W images with a peripheral rim of a high signal, is most often seen with neurofibromas (Fig. 8). Histologically, a central fibro-collagenous core and surrounding myxomatous tissue

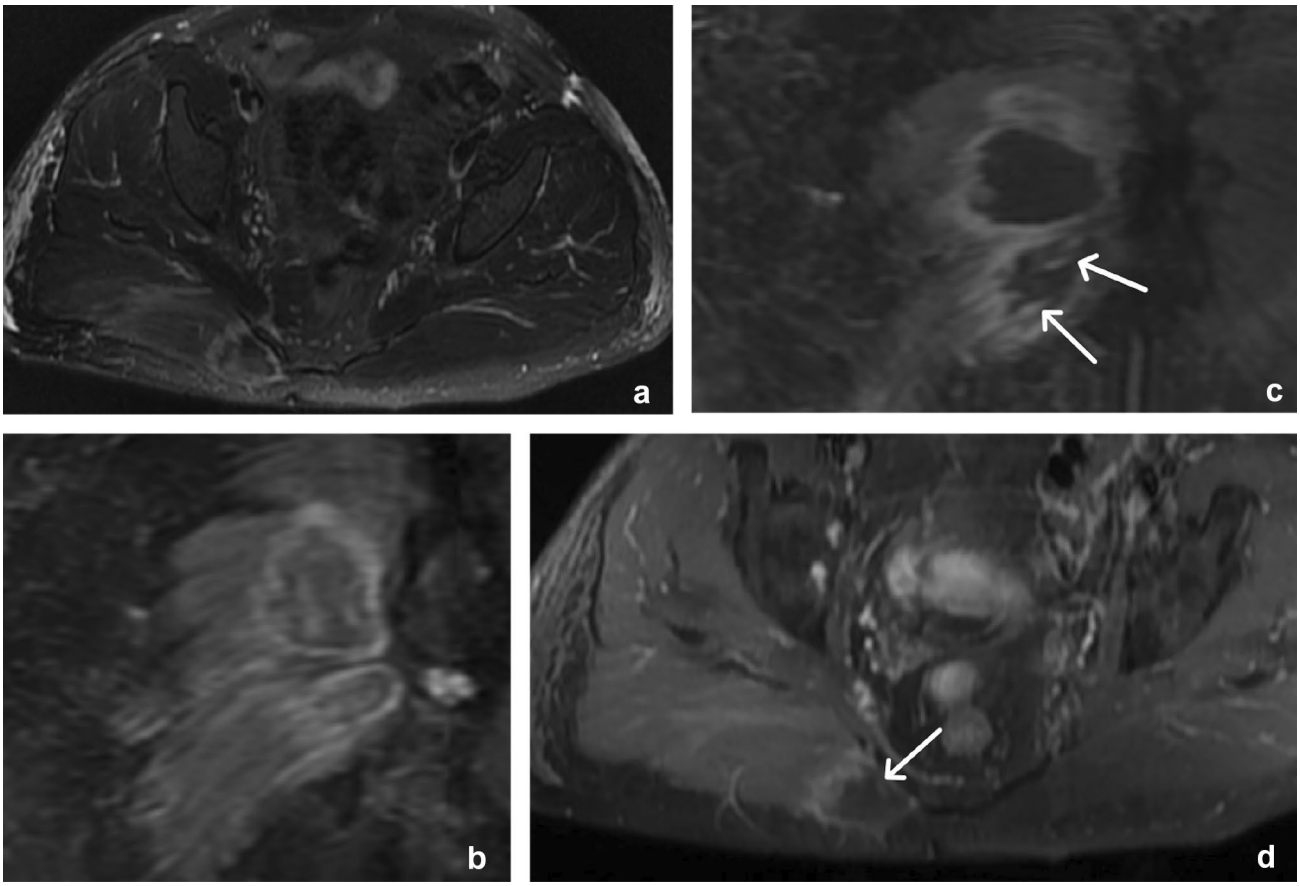

Fig. 3 47-year-old male with right gluteus maximus muscle myonecrosis. Axial T2 fat-saturated (**a**) and coronal STIR (**b**) MR images demonstrate heterogeneously increased signal, although less than fluid intensity, within and around the lesion. Coronal (**c**) and axial (**d**) post-contrast fat-saturated T1W MR images reveal rim enhancement as well as foci of internal enhancement (arrows), illustrating a subtle "stipple" sign

account for this imaging pattern. The target sign may also be seen in schwannomas; however, in these lesions, it is due to a central distribution of the more cellular Antoni type A cells, with a surrounding rim of hypocellular Antoni type B cells. Loss of a previously seen target sign in a peripheral nerve sheath tumor is concerning for malignant transformation. The tumor sometimes appears to have a "tail" on either side, representing the entering and exiting nerve [15, 16]. While these are benign tumors, they may exhibit locoregional mass effect and may show heterogeneous enhancement (Fig. 9).

Perineural (tarlov) cysts

Perineural cysts, eponymously known as Tarlov cysts, in contrast to neurofibromas, are cerebrospinal fluid (CSF) filled cysts of the nerve root sheath in the dorsal root ganglia of the lower spine. They are seen in up to 5% of the general population. They can be sporadic or associated with connective tissue disease. They are usually asymptomatic, but can be associated with back pain [17]. Imaging demonstrates classic findings for the diagnosis,

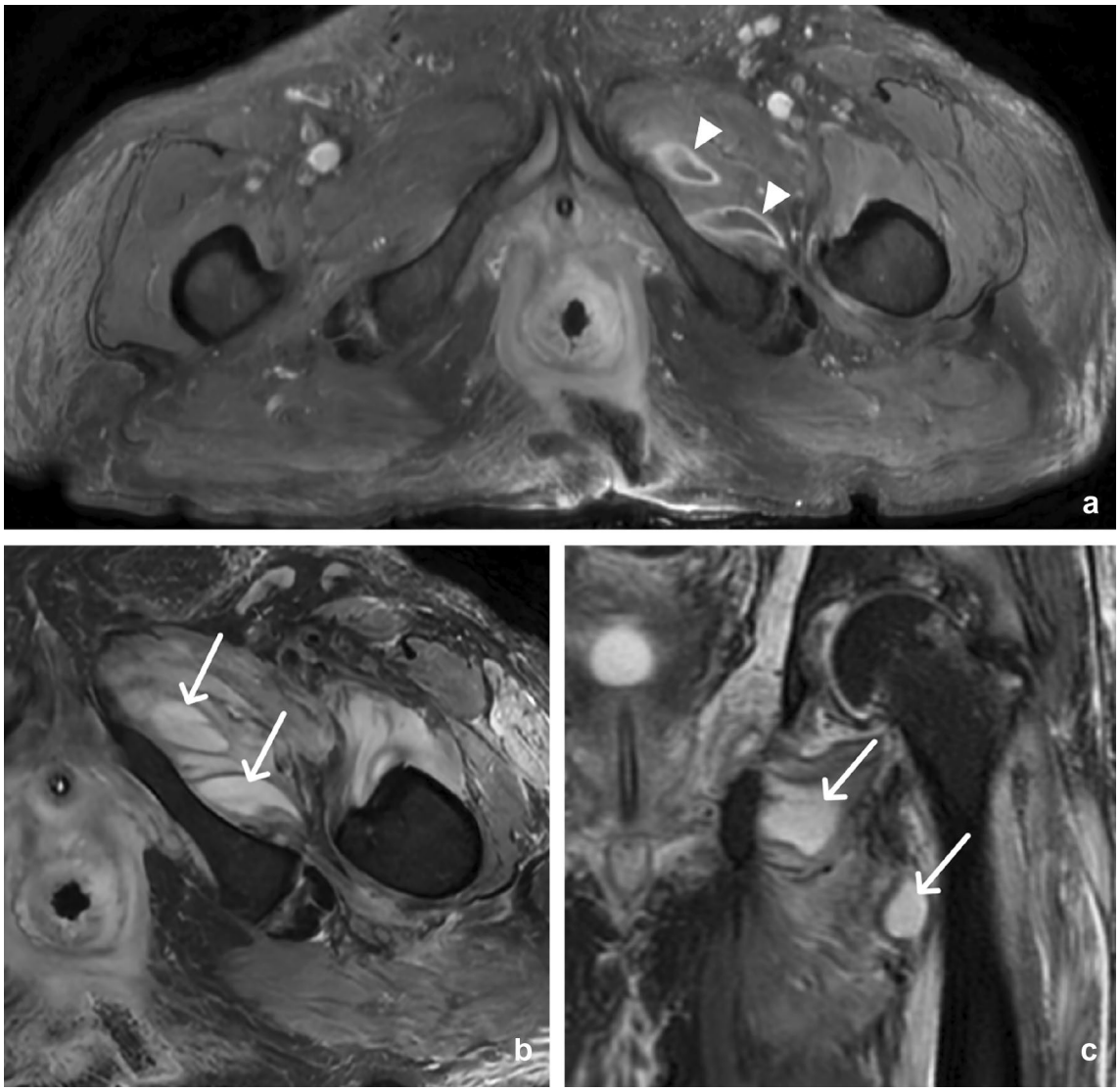

Fig. 4 62-year-old male with left adductor muscle intramuscular abscess. Axial post-contrast T1W (**a**) MR images demonstrate multiple rim enhancing lesions (arrowheads) with no internal enhancement. Axial (**b**) and coronal (**c**) T2W images demonstrate fluid signal hyperintensity within the lesions (arrows), helping to differentiate these as abscesses rather than myonecrosis or myositis

manifesting as simple cystic structures closely related to the lower lumbar and sacral dorsal ganglia and posterior nerve root junctions. Mild locoregional mass effect may be seen with remodeling of adjacent bone and enlargement of neural foramina. On unenhanced CT and MRI, these may mimic neurofibromas, but they will not enhance following intravenous (IV) contrast administration and will follow the CSF signal on all sequences of MRI (Fig. 10).

Filum terminale lipoma

The filum terminale is a fibrous strand of primarily pia mater, which extends from the conus medullaris (usually located at L1) to the periosteum of the coccyx and provides longitudinal support for the distal spinal cord. A filum terminale lipoma, also known as fatty filum terminale, is a common incidental finding in the lumbar

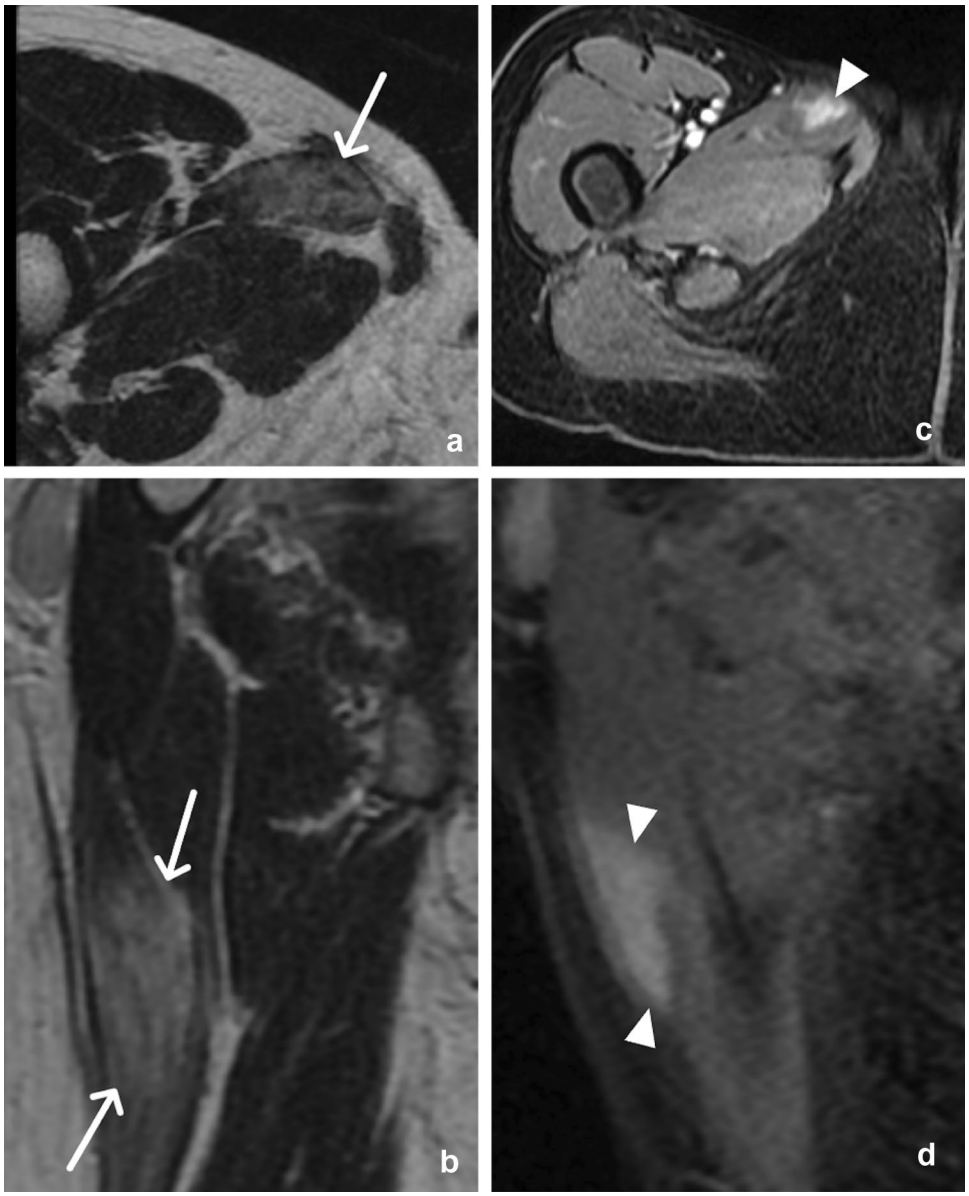

Fig. 5 46-year-old female with myositis. Axial (**a**) and sagittal (**b**) T2W MR images demonstrate heterogeneous mild hyperintensity in the right adductor longus muscle (arrows), compatible with edema. Axial (**c**) and sagittal (**d**) post-contrast fat-saturated T1W images reveal internal intramuscular enhancement (arrowheads), distinguishing this entity from myonecrosis or intramuscular abscess

spine, present in up to 4–6% of post-mortem exams [18], and is usually of no clinical concern; however, there may be an association with tethered cord syndrome. On CT imaging, a filum terminale lipoma will be seen as a fat density, linear, low-attenuating mass below the level of the conus medullaris (Fig. 11). MRI should be recommended if there are clinical signs of tethered cord. On MRI, the filum terminale lipoma will follow fat signal intensity on all sequences. Associated findings in support of tethered cord syndrome include filum thickening (> 2 mm) and a low-lying conus, at or below the midpoint of L2 [19–21].

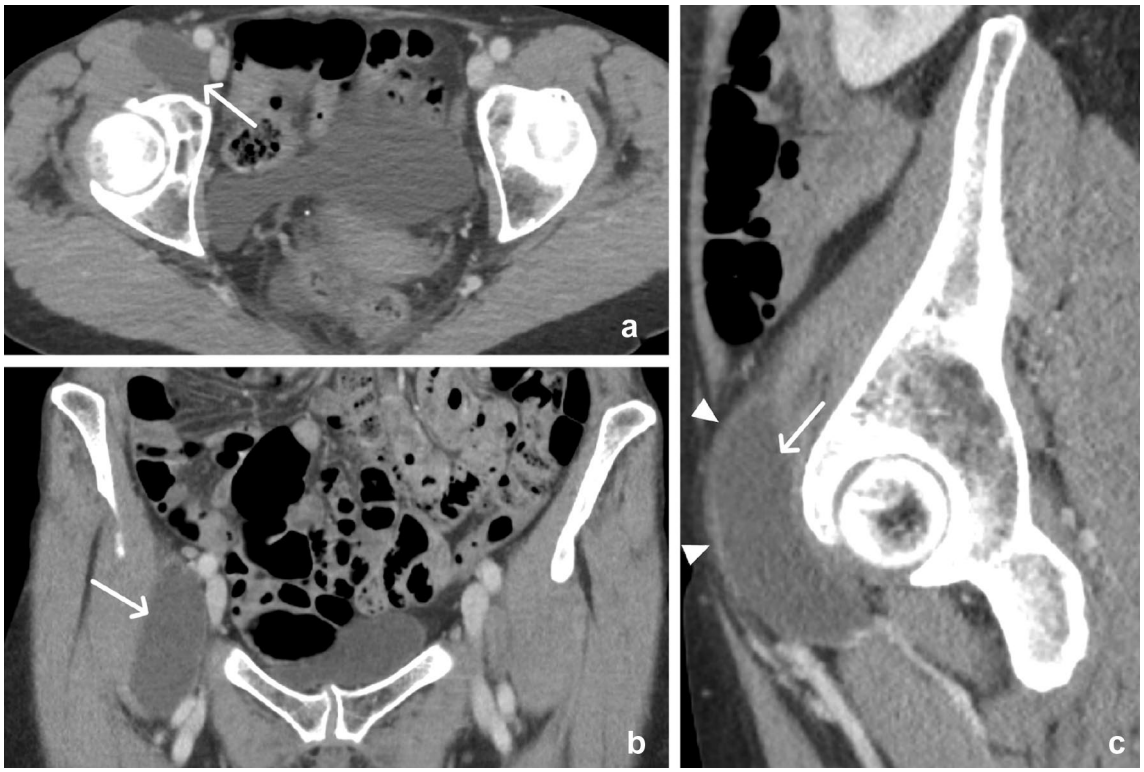

Fig. 6 65-year-old female with iliopsoas bursitis. Axial (**a**), coronal (**b**), and sagittal (**c**) CT images demonstrate a well-defined cystic structure (arrows) with a thin mildly enhancing wall (arrowheads) that lies anterior to the hip joint and posteromedial to the iliopsoas muscle

Subcutaneous lesions

Morel-Lavallée lesion

Morel-Lavallée (ML) lesions are post-traumatic subcutaneous cysts resulting from soft tissue degloving injury that classically occur over the greater trochanter of the femur and are caused by shear injury most commonly seen after tangential trauma, such as from motorcycle accidents. The skin and subcutaneous tissues separate from the underlying deep fascia, and serosanguinous fluid accumulates in the space created between these tissues and the fascia. This fluid collection may resolve spontaneously, or it may persist and become encapsulated with rim calcifications. On CT, one may see a smoothly contoured mass with pseudo-capsule and internal fluid attenuation predominating with fluid–fluid levels, if hemorrhage is present (Fig. 12). Classic MR features of ML lesions are variable in signal intensity, with partial or complete septations, fat globules, and fluid–fluid levels [22]. It is important for the radiologist to differentiate this entity from a simple subcutaneous or intramuscular hematoma, as an ML lesion may require acute to subacute treatment with drainage/debridement and if not treated may result in re-accumulation of fluid, infection, continued expansion, overlying tissue necrosis, or chronic pain, whereas soft tissue hematomas are typically managed conservatively. An ML lesion is located in the deeper subcutaneous tissues, near the deep fascial plane [23].

Sclerosing lipogranuloma

Injection of exogenous oils such as mineral, paraffin, or other foreign bodies commonly elicits a sclerosing lipogranulomatous reaction [24]. Non-contained silicone, often from

Fig. 7 20-year-old man with rectus abdominis muscle strain from abdominal crunches. Coronal CT (**a**) demonstrates bilateral low attenuation involving the rectus abdominis muscles (arrows). Coronal T2W (**b**), axial T1W (**c**), and axial T2W fat-saturated (**d**) MR images demonstrate corresponding increased T1 and T2 signal intensity (arrows), consistent with acute intra-muscular hemorrhage, which is hyperintense on both sequences

ruptured implants or injected free-silicone, tends to form granulomas, fibrosis, and will occasionally migrate [25]. On CT, it appears as diffuse thickening of superficial and deep soft tissues infiltrated with multiple locules containing macroscopic fat deposits (Figs. 13 and 14).

Liposuction

Liposuction is one of the most common cosmetic procedures performed internationally for reshaping the body contour [26]. The abdominal wall is made up of multiple layers from superficial to deep, including the skin, subcutaneous adipose tissue, Scarpa fascia, muscles, investing deep fascia, transversalis fascia, and the peritoneum [27]. Suction assisted liposuction involves making a small skin incision, inserting a blunt cannula attached to a vacuum, and using multiple repeated strokes with the cannula to aspirate fat from the deep subcutaneous layer, sometimes with the administration of water or vasoconstrictive substances to minimize blood loss [28, 29]. Expected findings include infiltrative soft tissue or fluid attenuation within the deep subcutaneous fat and possible subcutaneous emphysema. Thin radiating

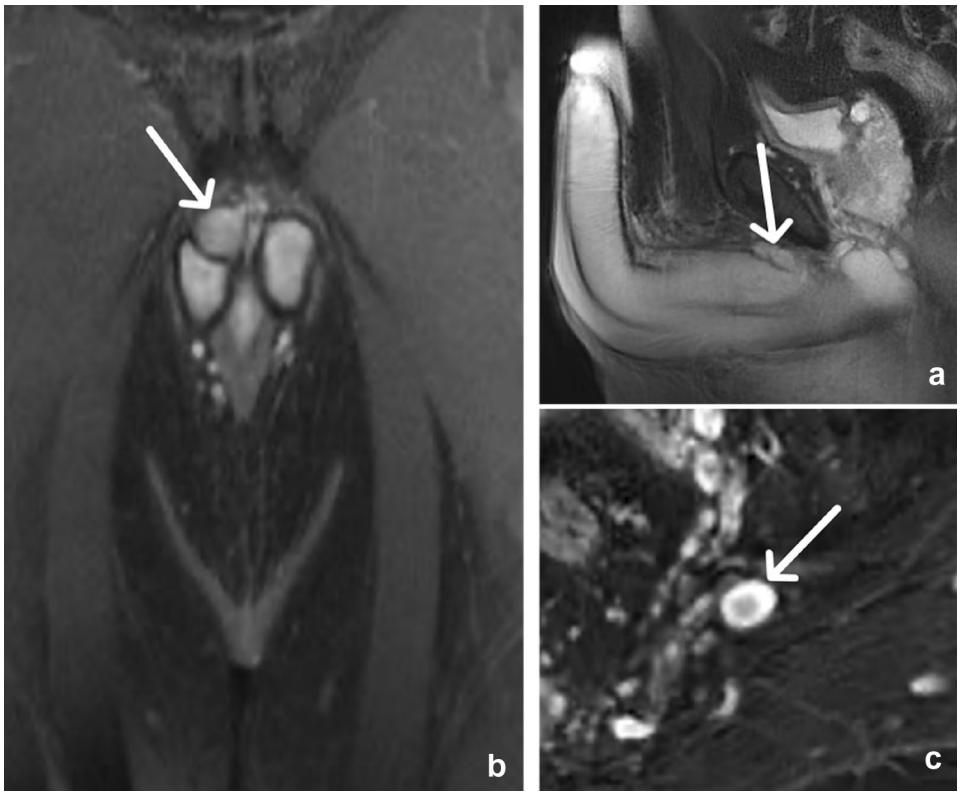

Fig. 8 36-year-old male with Neurofibromatosis type I demonstrating a penile and multiple additional sacral neurofibromas. Sagittal (**a**) and coronal (**b**) T2W fat-saturated MR images demonstrate an elongated mass with high signal intensity in the dorsal aspect of the penis (arrow). Axial (**c**) T2W fat-saturated images reveal additional ovoid masses of the sacral plexus which demonstrate the "target sign" appearance, with high peripheral signal intensity and low central intensity (arrow)

linear lesions perpendicular to the skin and thicker linear lesions parallel to the skin representing cannula insertion tracks are also commonly seen [29, 30]. Complications of liposuction include cellulitis, abscess formation, necrotizing fasciitis, and vascular or lymphatic injury, which may result in hematoma or lymphocele development [31]. Here, we present a case of a 25-year-old female who recently underwent abdominal liposuction to demonstrate normal post-procedural CT findings (Fig. 15) as well as a 33-year-old female with pre- and post-procedural imaging for comparison (Fig. 16).

Transverse rectus abdominis muscle flap

Transplantation of a transverse rectus abdominis muscle (TRAM) flap is a common surgical procedure post-mastectomy. Originally described by Hartrampf et al. [32] in 1982, the technique has evolved to include pedicled, free, and delayed flap reconstructions. The rectus abdominis muscle is supplied by both the superior epigastric artery and the more robust inferior epigastric artery. In a pedicled TRAM flap reconstruction, the superior epigastric arterial supply is utilized, requiring the entire length of the rectus abdominis muscle to be transplanted. The rectus abdominis muscle and associated lower abdominal soft tissues are subcutaneously tunneled into the mastectomy surgical site. A portion of the abdominal epidermis is utilized to create the neobreast skin surface, while the remainder is de-epithelialized [33]. In contradistinction to a pedicled flap, a free TRAM flap reconstruction utilizes the more robust inferior epigastric arterial supply. The inferior epigastric vessels are dissected, transplanted, and re-anastomosed in the chest to the thoracodorsal, subscapular, or internal mammary artery and vein. This approach may be preferred in patients with atherosclerotic vascular risk factors [33]. Since less of the

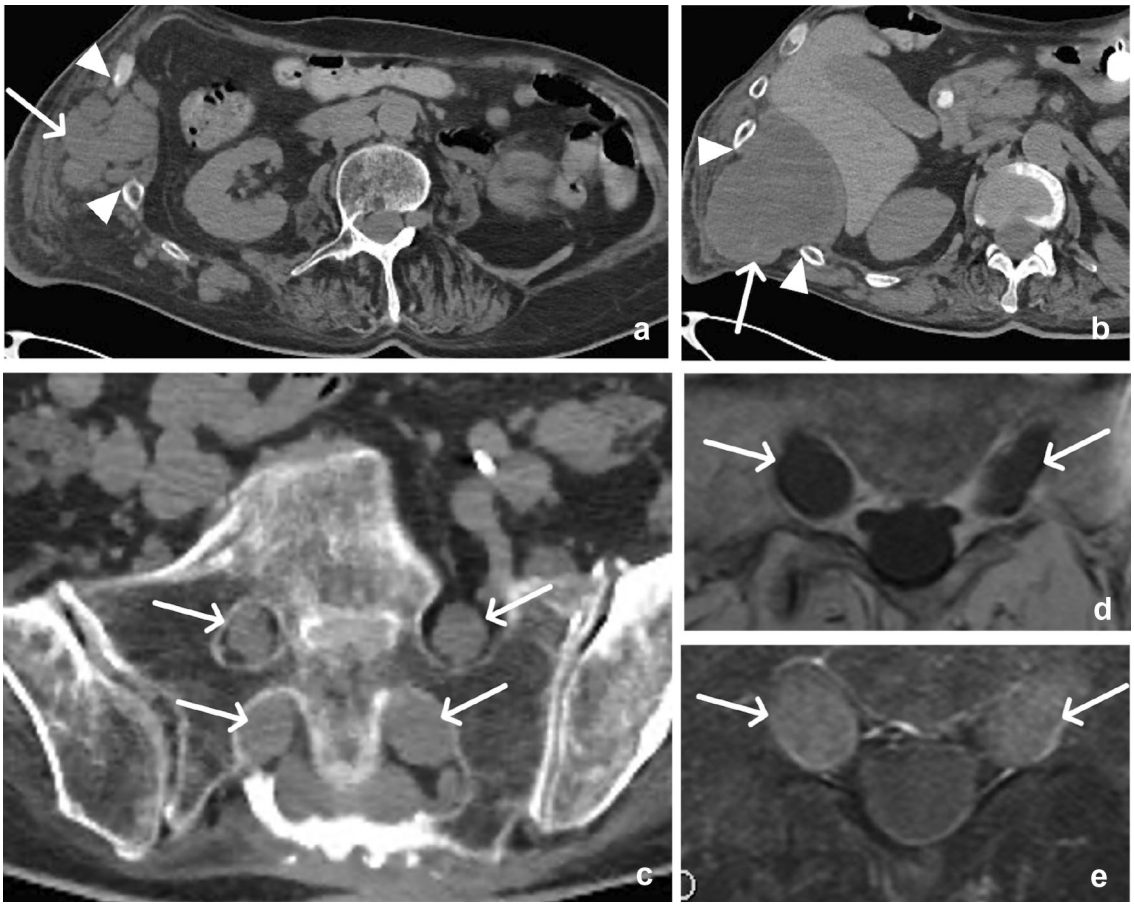

Fig. 9 46-year-old male with Neurofibromatosis type I demonstrating chest wall and sacral neurofibromas. Axial CT images (**a**, **b**) demonstrate soft tissue masses (arrow) in the posterolateral chest wall with widening of the intercostal spaces (arrowheads) and smooth remodeling of the adjacent costal margins. Axial CT through the sacrum (**c**) shows bilateral and symmetric intermediate attenuation masses in the sacral foramina (arrows). Axial T1W pre- (**d**) and post-contrast (**e**) MR images through the sacrum demonstrate enhancement of these lesions (arrows)

rectus abdominis muscle is harvested in a free flap, there is a decreased risk of associated adnominal wall hernia.

The most common imaging findings include replacement of normal glandular breast tissue with subcutaneous fat, the presence of an atrophied rectus abdominis muscle anterior to the chest wall, the absence of some or all of the rectus abdominis musculature along the anterior abdominal wall, and associated surgical clips, most prominent in the lower anterior abdominal wall [34]. Here, we present a case of a patient with breast cancer who underwent bilateral mastectomies, followed by pedicled TRAM flap reconstruction (Figs. 17 and 18).

Calvarial bone flap

Decompressive craniectomy is a neurosurgical approach to treat uncontrolled elevated intracranial pressure. Surviving patients require a cranioplasty after the acute episode of intracranial swelling has resolved. One approach to cranioplasty is to preserve the resected portion of cranium and reimplant it as an autologous bone flap. The resected bone may be stored in a cryopreservation freezer (ex vivo) or in a subcutaneous pocket within the patient themselves (in vivo) [35]. The most common risks associated with either technique include infection and osseous resorption.

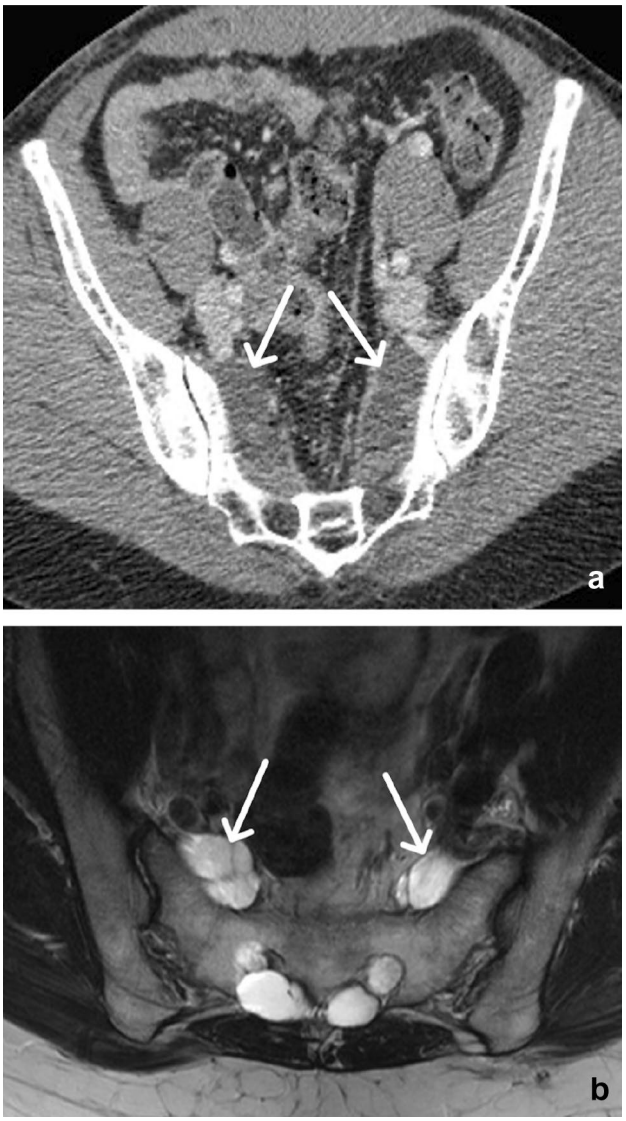

Fig. 10 42-year-old male with perineural (Tarlov) cysts. Axial contrast-enhanced CT (**a**) and T2W MR (**b**) images demonstrate CSF attenuation and signal intensity in simple cystic structures closely related to the sacral and lower lumbar nerves without evidence of enhancement (arrows). The sacral foramina are mildly enlarged

Multiple studies have shown no convincing difference in rates of either between in vivo or ex vivo storage of autologous calvarial bone flaps in most patients [36–38]; however, one retrospective review found lower rates of infection with in vivo preservation in patients with traumatic brain injury [38]. We present a case of a 50-year-old female with a history of a recent traumatic subdural hematoma status post-decompressive craniectomy at an outside institution who presented with right lower quadrant pain. An osseous structure, corresponding to a removed calvarial fragment seen on head CT, can be seen in the subcutaneous tissues in the right lower abdominal wall with surrounding hematoma and internal foci of gas (Fig. 19).

Subcutaneous panniculitis (erythema nodosum)

Panniculitis is a nonspecific histopathologic term to describe inflammation of adipose tissue. Panniculitis most commonly affects subcutaneous fat; however, intra-abdominal forms such as mesenteric panniculitis are widely recognized. There are many etiologies for panniculitis, including inflammation, infection (including COVID-19 infection), trauma, and malignancy, among others [39, 40]. On CT imaging, increased attenuation and "fat stranding" may be seen within the subcutaneous adipose tissues, consistent with the clinical diagnosis of erythema nodosum (Fig. 20).

Hidradenitis suppurativa

Hidradenitis suppurativa (HS) is a chronic inflammatory skin disease involving the folliculopilosebaceous units and apocrine sweat glands and is also known as acne inversa. It has a female predominance and is associated with obesity, smoking, Crohn's disease, and Dowling Degos disease and may be complicated by chronic sinus and fistula formation, epidural abscess from deep extension, osteomyelitis, and squamous cell carcinoma developing in chronic inflammatory tracts [41–43].

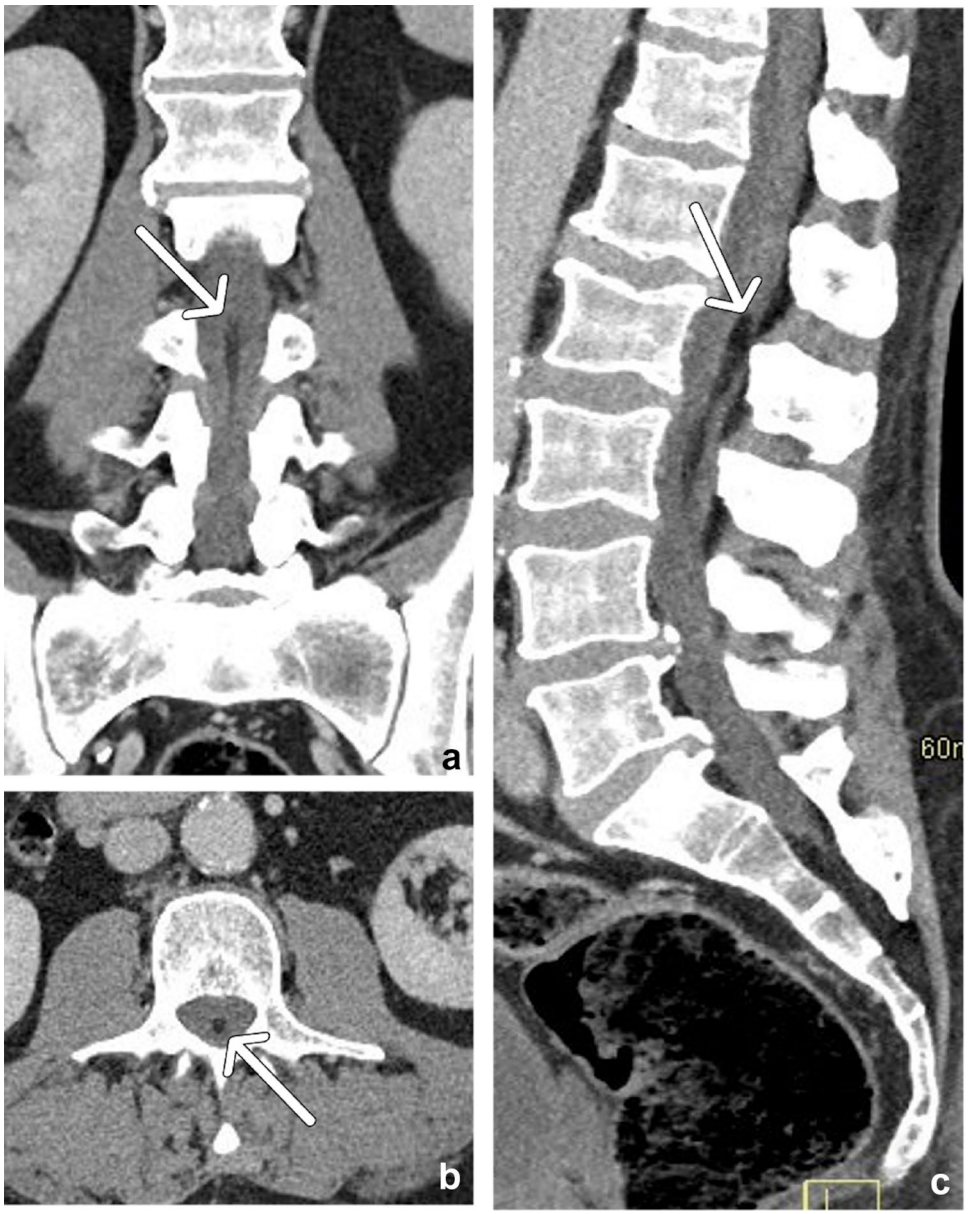

Fig. 11 63-year-old male with a filum terminale lipoma. Coronal (**a**), axial (**b**), and sagittal (**c**) CT reformats demonstrate a linear region of fat attenuation (arrows) at the base of the conus medullaris extending from L2 to L3, along the filum terminale, representing a filum terminale lipoma. The patient had no clinical signs of tethered cord syndrome

The disease typically affects apocrine gland-rich areas of the body, such as the genitofemoral area and axillae [42]. Imaging shows marked thickening of the skin, edema of the subcutaneous tissues, and formation of multiple small subcutaneous abscesses as well as sinus and fistula formation. It has a characteristic distribution, causing severe skin thickening which is typically bilateral and fairly symmetric along the perineum and gluteal folds (Fig. 21) or the axillary folds [44]. By comparison, simple cellulitis tends to have a more diffuse "fat stranding" appearance with more mild skin thickening. The involved areas are typically of soft tissue attenuation on CT, dark on T1, and bright on T2-weighted MR images with peripheral enhancement of subcutaneous abscesses (Fig. 22). MR imaging can be very helpful when HS involves the genitofemoral areas in patients with Crohn's disease (who have an increased incidence of HS) to determine the cause of a peri-anal fistula, which can occur in both Crohn's disease and HS. A recent study showed that while some MRI features of anoperineal disease may overlap between Crohn's disease and HS, a specific diagnosis of HS is possible with a combination of three features: absence of perianal predominance of disease, absence of rectal wall thickening, and bilaterality of features [45].

Fig. 12 46-year-old male with a Morel-Lavallée lesion. Axial CT demonstrates a left lateral upper thigh fluid filled encapsulated collection (arrow) with rim calcification (arrowhead) located superficial to the deep fascia and deep to the subcutaneous fat

Congenital and developmental lesions

Hydrocele of canal of nuck

Hydrocele of the canal of Nuck is a rare condition in female children. The processus vaginalis is a normal embryologic structure representing an outpouching of the parietal peritoneum through the inguinal canal into the labia majora, which normally obliterates between the seventh month of gestation and 1 year of age. Failure to close results in a continued outpouching known as the canal of Nuck[46]. This rare entity is associated with prematurity, with an overall incidence of < 1%[47, 48], but occurring in 9–11% of premature infants[49]. Complications include hydrocele and indirect hernia of the bowel or pelvic organs, which may result in incarceration and strangulation of bowel or ovarian torsion within the canal[46]. MRI demonstrates an ovoid fluid-filled structure, typically with high signal intensity on

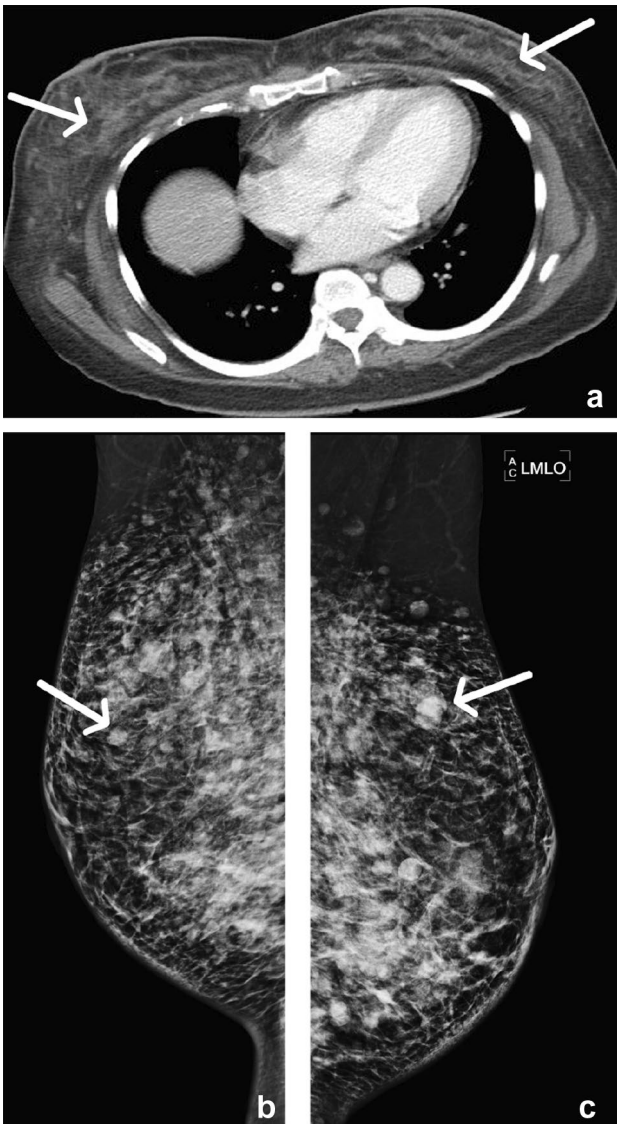

Fig. 14 30-year-old female with sclerosing lipogranulomas. Axial CT (**a**) images demonstrate heterogenous material in the superficial and deep adipose tissue of the breasts (arrows). Bilateral mammogram images (**b**, **c**) demonstrate numerous small dense masses with rim calcifications (arrows), a recognized pattern of free silicone injection

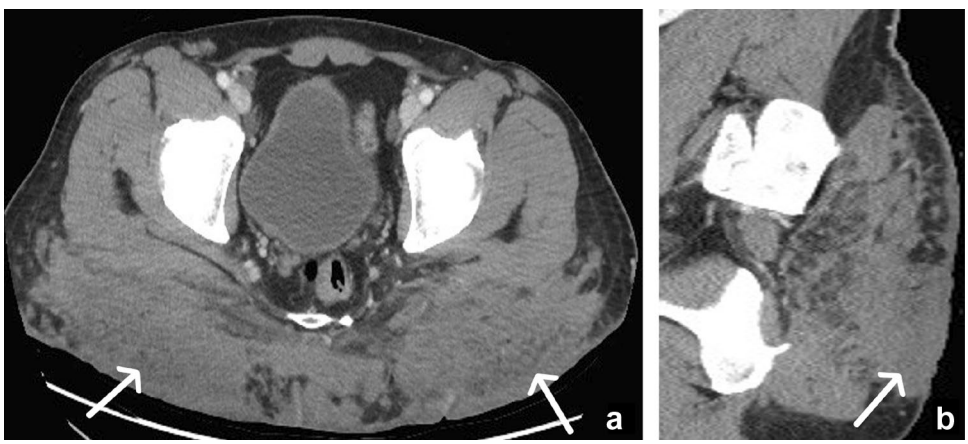

Fig. 13 29-year-old female with sclerosing lipogranulomas. Axial (**a**) and sagittal (**b**) CT images demonstrate diffuse thickening of the superficial and deep subcutaneous tissues (arrows) infiltrated with multiple locules containing macroscopic fat deposits

Fig. 15 25-year-old female with recent abdominal liposuction. Axial CT of the lower abdomen demonstrates a curvilinear soft tissue attenuating lesion tracking circumferentially about the patient in the subcutaneous fat parallel to the skin (arrows). This is a normal finding in the post-liposuction setting and represents cannula insertion tracks

T2W imaging and low to moderate signal on T1W imaging in the inguinal canal (Fig. 23).

Klippel-Trenaunay-Weber syndrome

With an incidence of 1 out of 275,000 births, Klippel-Trenaunay-Weber Syndrome (KTS) is a sporadic, rare, congenital syndrome characterized by port-wine stain (nevus flammeus), vascular malformations (varicosities and hemangiomas), asymmetric appendicular bone, and soft tissue hypertrophy. Only two of the three criteria need to be present to make a diagnosis KTS. The involvement of the gastrointestinal and genitourinary systems is not uncommon. Routine CT can detect enlargement of the extremity with bone elongation and circumferential soft tissue hypertrophy, subcutaneous varicose veins, phleboliths, and capillary

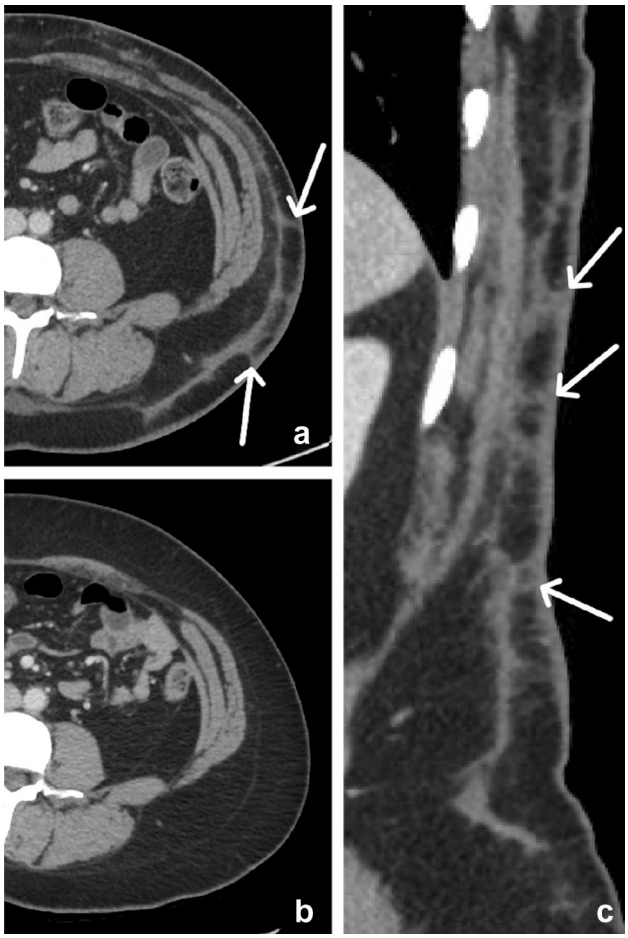

Fig. 16 33-year-old female with abdominal wall liposuction 3 weeks prior. Axial (**a**) and sagittal (**c**) images demonstrate, thinner radiating lesions perpendicular to the skin (arrows) in addition to the thick curvilinear lesions parallel to the skin, both likely representing cannula insertion tracks. Axial pre-operative (**b**) CT image is provided for comparison

malformation suggesting the diagnosis (Fig. 24). MRI and MR angiography (MRA) are beneficial to evaluate vascular malformation preoperatively [50].

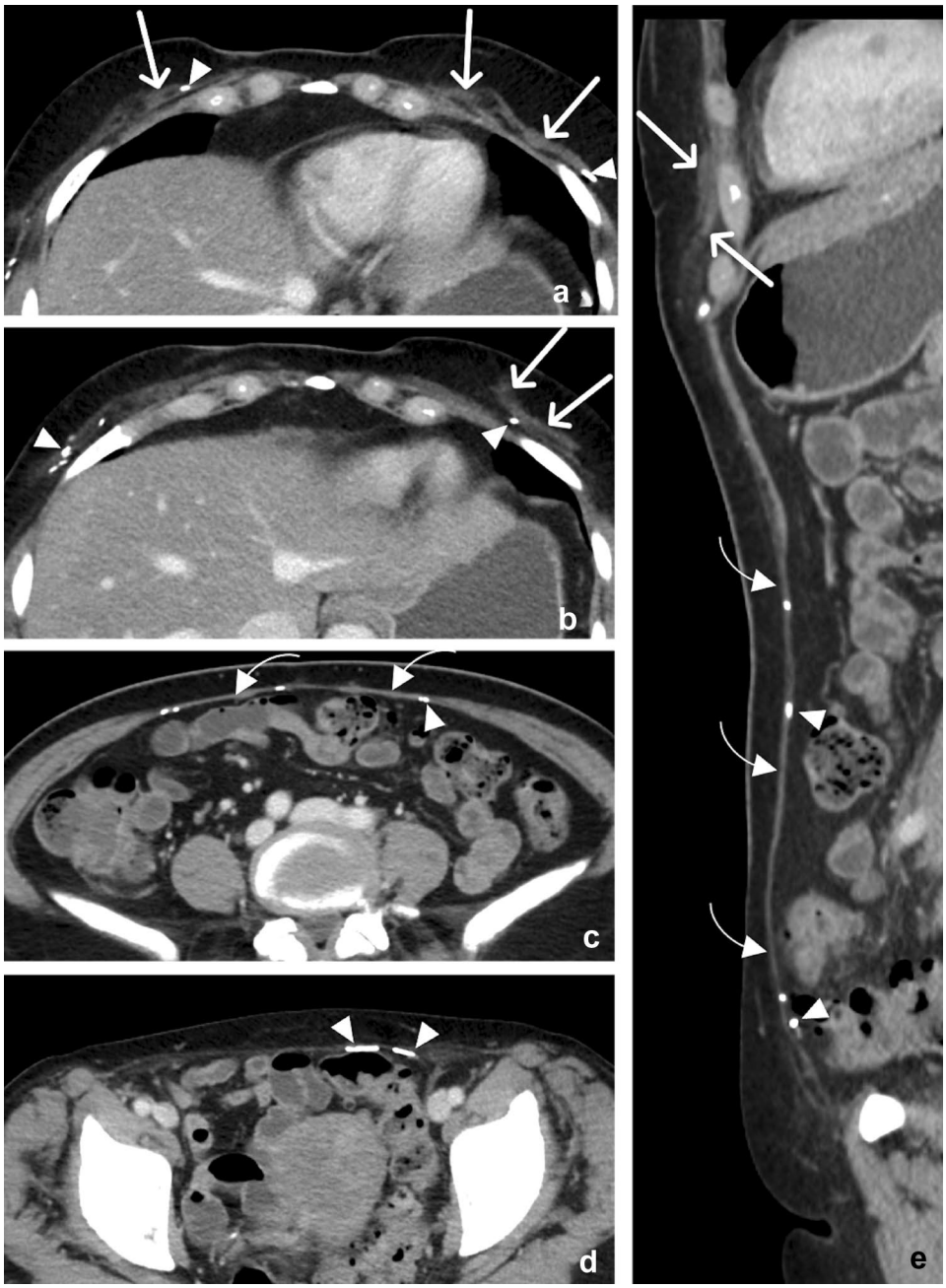

Fig. 17 69-year-old female with bilateral transverse rectus abdominis muscle (TRAM) flap reconstruction after bilateral mastectomy. Axial images from the lower chest to the pelvis (**a**, **b**, **c**, **d**) and sagittal (**e**) CT images and demonstrate absent rectus abdominis muscle along the anterior abdominal wall (curved arrow), which is seen atrophied and transplanted along the left anterior chest wall (arrows). Scattered surgical clips are present (arrowheads). Note the absence of glandular tissue in the breasts

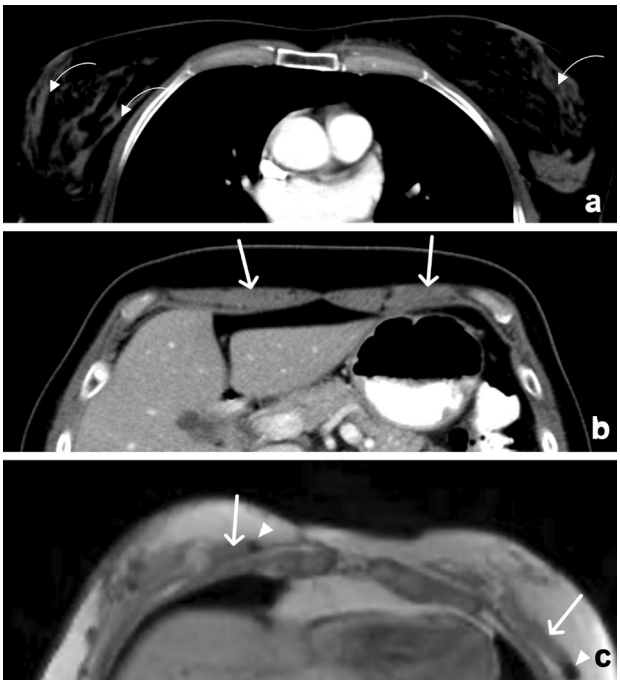

Fig. 18 Preoperative CT and postoperative MRI correlate for Fig. 17. Axial CT (**a**) demonstrates the presence of normal glandular breast tissue (curved arrows). Axial CT (**b**) illustrates the normal rectus abdominis muscles (arrows) shortly before the TRAM flap procedure. Axial T1W MR (**c**) demonstrates bilateral transplanted rectus abdominis muscles (arrows), a few foci of susceptibility related to surgical clips (arrowheads), and a paucity of glandular tissue

Miscellaneous

Chronic iliac subperiosteal hematoma

Subperiosteal ossified hematomas of the iliac bone have been reported in the orthopedic literature as uncommon post-traumatic lesions that specifically occur in young patients [51]. They are typically caused by vigorous sports activity in adolescence and may be clinically indolent and usually incidentally detected in patients examined for other reasons. These lesions appear on CT as lens shaped lesions on the medial aspect of the iliac bone containing bone marrow with a dense line between the ossified subperiosteal hematoma and the iliac bone marrow called the 'ghost native cortex' (Fig. 25). The presence of the ghost native cortex between the native marrow of the iliac bone and the marrow of the ossified subperiosteal hematoma helps distinguish from fibrous dysplasia which can otherwise have a similar appearance [52]. On MRI, it appears as a mildly enhancing T1-low, T2-high signal intensity lesion without abnormal bone marrow edema, periosteal reaction, or perilesional soft tissue edema [51, 53]. This entity should not be mistaken for an aggressive intraosseous lytic lesion and identification of the pathognomonic 'ghost native cortex' sign can help avoid additional unnecessary workup.

Fig. 19 50-year-old female with a subcutaneous bone flap after decompressive craniotomy for a traumatic subdural hematoma. Axial (**a**), coronal (**c**), and sagittal (**d**) contrast-enhanced CT images demonstrate a curvilinear osseous structure (arrows) in the subcutaneous tissues of the right lower quadrant with surrounding hematoma and foci of gas (arrowheads). This corresponds to a missing fragment of the calvarium seen on axial head CT (**b**). In fact, the coronal suture can be seen on sagittal reconstructions (**d**) (arrow)

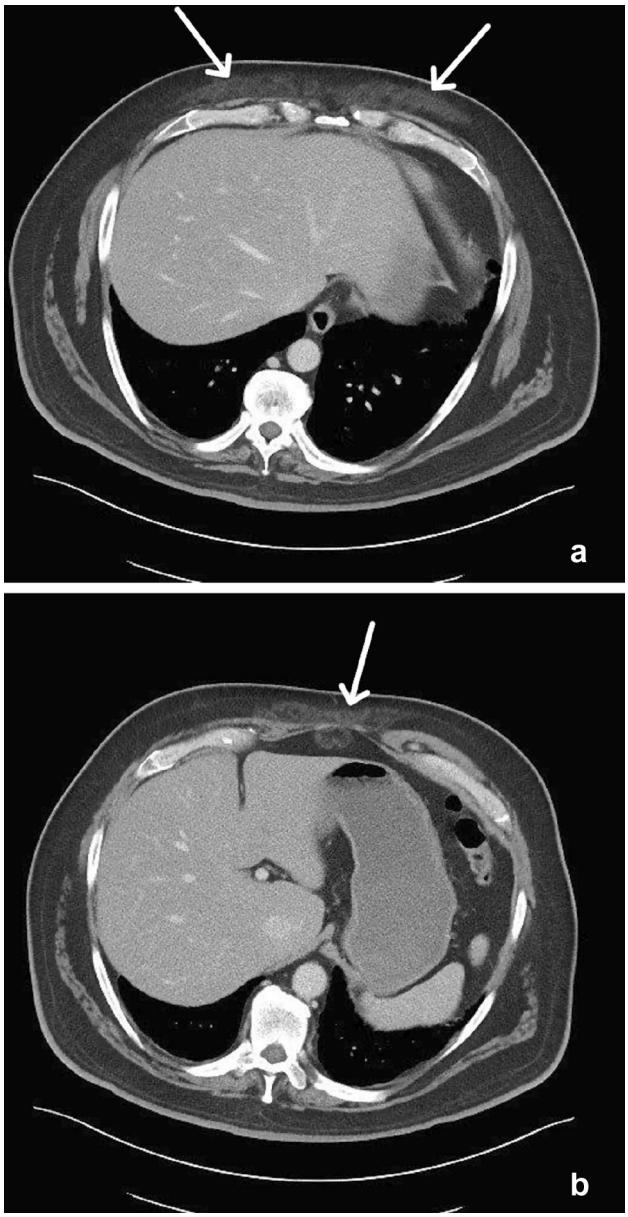

Fig. 20 52-year-old male with subcutaneous panniculitis. Two axial (**a**, **b**) CT images through the upper abdomen demonstrate increased attenuation and inflammatory changes in the anterior abdominal wall subcutaneous fat (arrows), consistent with subcutaneous panniculitis

Conclusion

Evaluation of extra-cavitary soft tissue abnormalities tends to be underemphasized in the interpretation of abdominal and pelvic CT and MR studies. We have presented a broad review of abdominal wall and spinal soft tissue findings encountered in our practice with pearls from the current knowledge about interpretation and management in order to improve awareness of these entities.

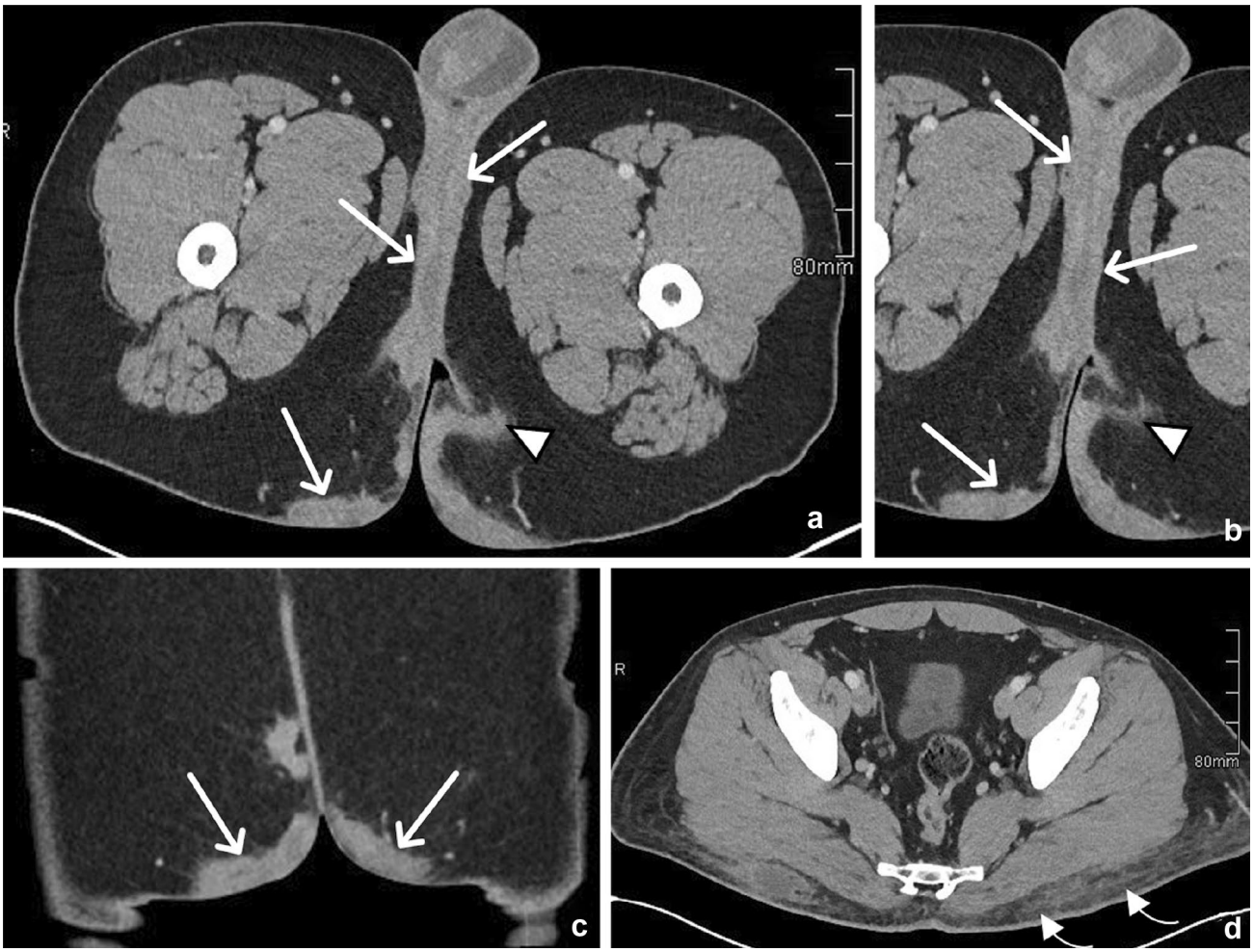

Fig. 21 30-year-old male with Hidradenitis Suppurativa (HS). Axial (**a**, **b**) and coronal (**c**) CT reformats through the gluteal cleft and perineum demonstrate nodular, bilateral, fairly symmetrical subcutaneous soft tissue thickening (arrows) with sinus track formation (arrowhead) in a patient with pathologically proven HS. Contrast these findings with a different patient with cellulitis. Axial (d) CT image illustrates diffuse "fat stranding" in the left greater than right gluteal subcutaneous soft tissues (curved arrows), compatible with cellulitis. A developing fluid collection is noted in the right gluteal subcutaneous tissues

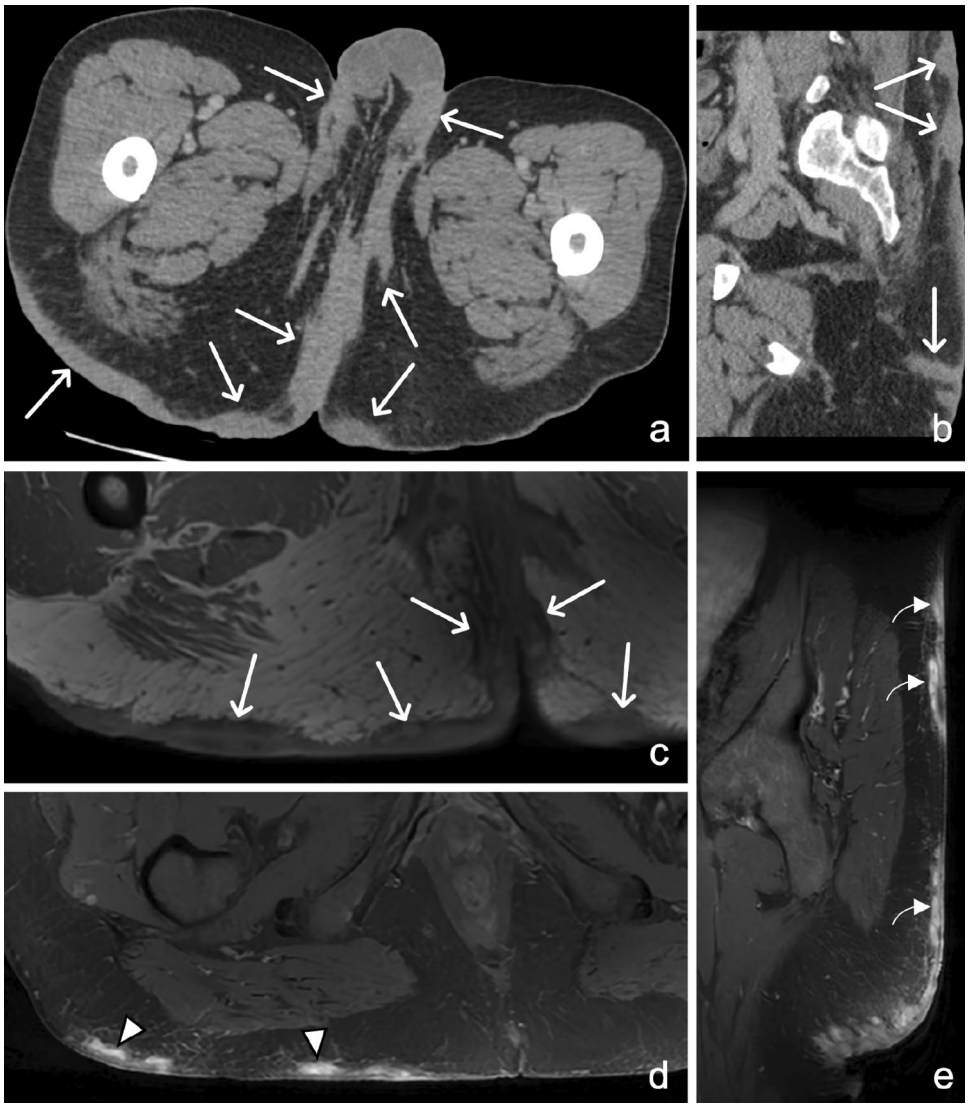

Fig. 22 49-year-old male with Hidradenitis Suppurativa (HS). Axial CT (**a**), sagittal CT (**b**), axial T1W (**c**), axial T2 fat-saturated (**d**), and sagittal post-contrast fat-saturated T1W (**e**) MR sequences demonstrate diffuse nodular skin thickening (arrows) along the scrotum, bilateral groin, medial thighs, posterior buttocks, and lower back with linear high T2 signal suggestive of sinus tracks (arrowheads) and areas of superimposed enhancement which may represent superimposed infection or micro abscesses (curved arrows)

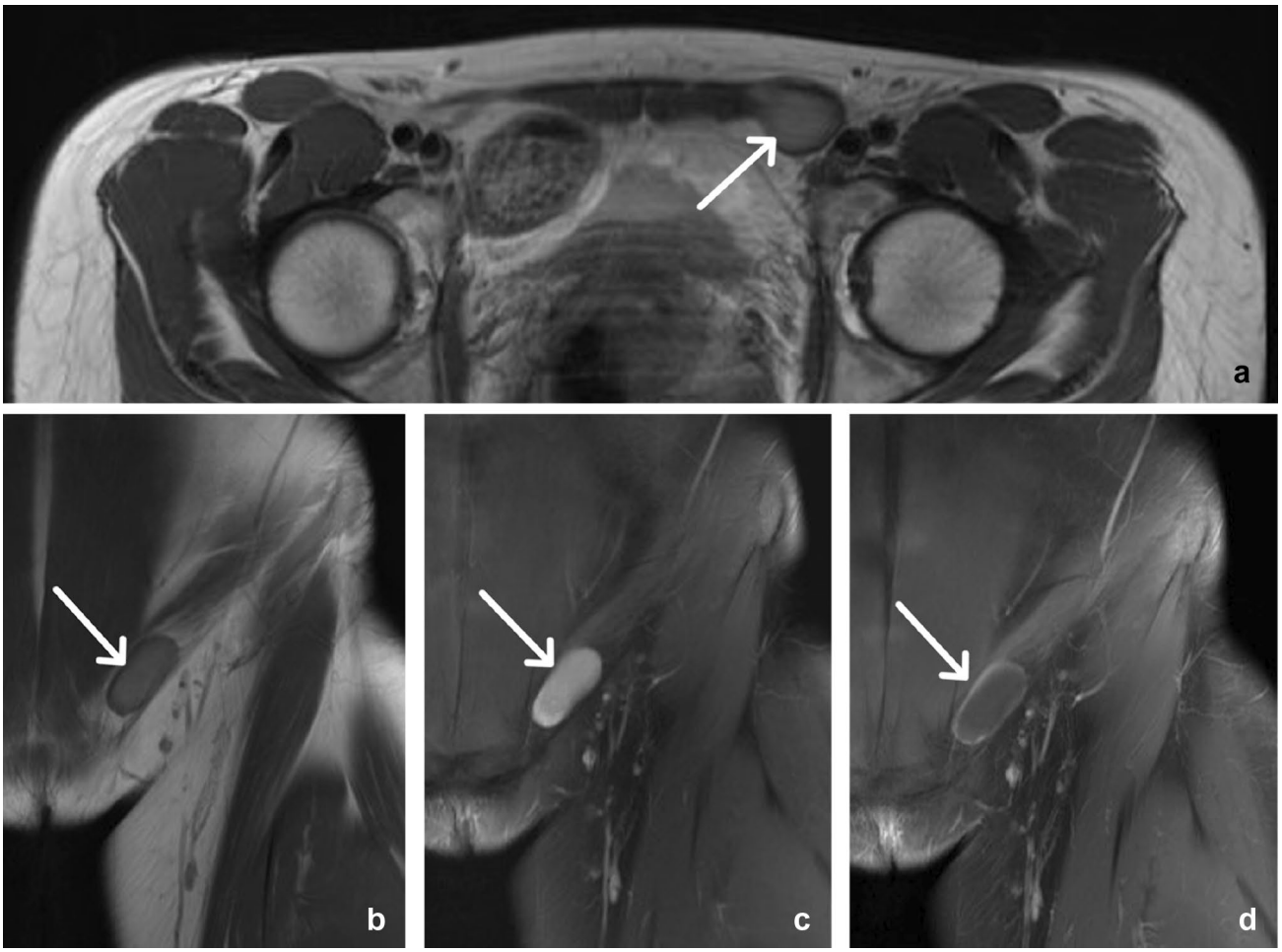

Fig. 23 32-year-old female with a Canal of Nuck hydrocele. Coronal T1 (**a**), coronal T2W fat-saturated (**b**), and axial T1W (**c**) images demonstrate an ovoid, simple fluid intensity structure within the left inguinal canal. Coronal T1W fat-saturated post-contrast (**d**) images demonstrate trace peripheral enhancement with no internal enhancement

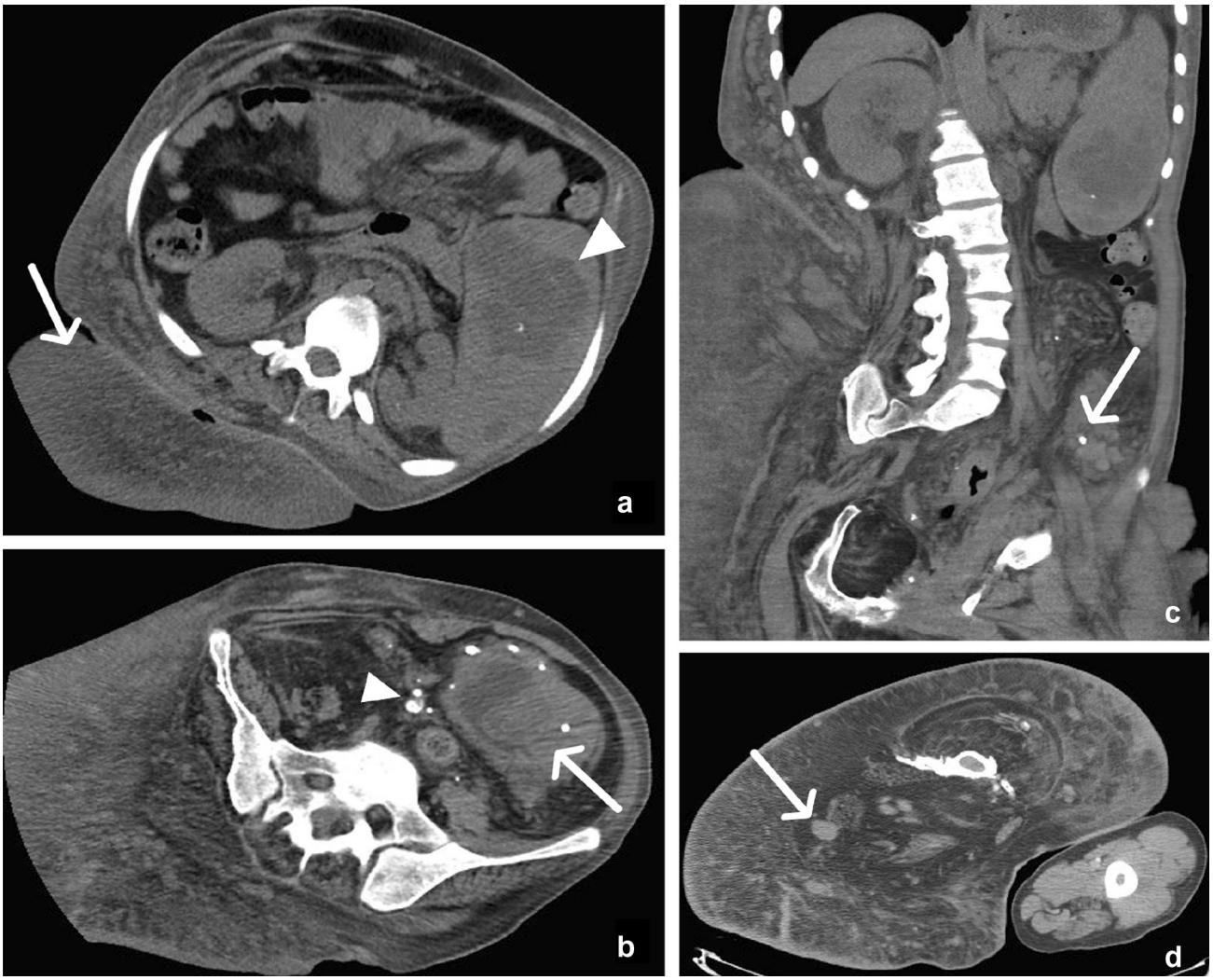

Fig. 24 30-year-old male with Klippel-Trenaunay-Weber Syndrome. Axial mid-abdomen CT (**a**) images demonstrate enlargement of the subcutaneous tissue of the right flank (arrow) and large splenic hemangioma (arrowhead). Axial pelvic CT (**b**) images show mesenteric venous malformations associated with phleboliths (arrowhead) and colonic hemangiomatosis with phleboliths (arrow). Coronal posterior abdomen CT (**c**) images show splenic and mesenteric hemangiomas with associated calcifications (arrow). Axial upper thigh CT (**d**) images demonstrate gigantism of the right lower extremity with soft tissue hypertrophy and numerous subcutaneous varicose veins (arrow)

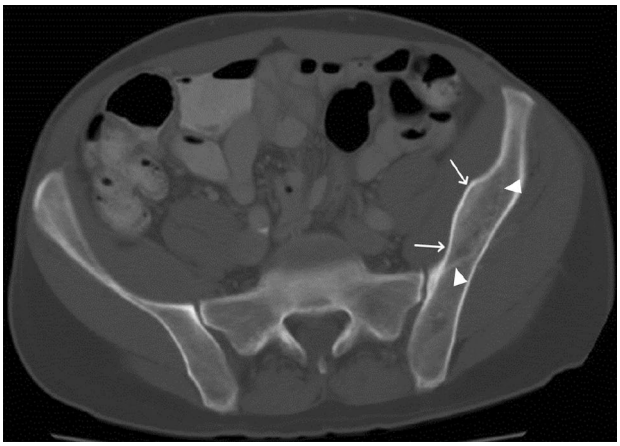

Fig. 25 20-year-old male with a chronic ossified subperiosteal hematoma of the left iliac bone. Axial pelvic CT images show a lens-shaped, expansile mass in the medial aspect of the left iliac bone with peripheral ossification (arrow). Note the dense line representing the native cortex of left iliac bone, termed the "ghost native cortex" sign (arrowheads)

Declarations

Competing interests The authors have no financial or non-financial disclosures.

References

1. Nguyen M, Beaulieu C, Weinstein S, Shin LK. The incidental bone lesion on computed tomography: management tips for abdominal radiologists. Abdom Radiol (NY). 2017; 42(5):1586-1605.https://doi.org/10.1007/s00261-016-1040-0
2. Bernard S, Walker E, Raghavan M. An Approach to the Evaluation of Incidentally Identified Bone Lesions Encountered on Imaging Studies. AJR Am J Roentgenol. 2017; 208(5):960-970.https://doi.org/10.2214/ajr.16.17434
3. Gaetke-Udager K, Girish G, Kaza RK, Jacobson J, Fessell D, Morag Y, et al. MR imaging of the pelvis: a guide to incidental musculoskeletal findings for abdominal radiologists. Abdom Imaging. 2014; 39(4):776-796.https://doi.org/10.1007/s00261-014-0108-y
4. Ballard DH, Mazaheri P, Oppenheimer DC, Lubner MG, Menias CO, Pickhardt PJ, et al. Imaging of Abdominal Wall Masses, Masslike Lesions, and Diffuse Processes. RadioGraphics. 2020; 40(3):684-706.https://doi.org/10.1148/rg.2020190170
5. Linton O. Edward B. D. Neuhauser. J Am Coll Radiol. 2011; 8(12):882.https://doi.org/10.1016/j.jacr.2011.03.008
6. Applegate KE, Neuhauser DVB. Whose Aunt Minnie? Radiology. 1999; 211(1):292-292.https://doi.org/10.1148/radiology.211.1.r99ap22292
7. Hall FM, Griscom NT. Gestalt: Radiology's Aunt Minnie. American Journal of Roentgenology. 2008; 191(4):1272-1272.https://doi.org/10.2214/AJR.08.1330
8. Baker JC, Demertzis JL, Rhodes NG, Wessell DE, Rubin DA. Diabetic Musculoskeletal Complications and Their Imaging Mimics. RadioGraphics. 2012; 32(7):1959-1974.https://doi.org/10.1148/rg.327125054
9. Cunningham J, Sharma R, Kirzner A, Hwang S, Lefkowitz R, Greenspan D, et al. Acute myonecrosis on MRI: etiologies in an oncological cohort and assessment of interobserver variability. Skeletal Radiol. 2016; 45(8):1069-1078.https://doi.org/10.1007/s00256-016-2389-4
10. Palmer W, Bancroft L, Bonar F, Choi JA, Cotten A, Griffith JF, et al. Glossary of terms for musculoskeletal radiology. Skeletal Radiol. 2020; 49(Suppl 1):1-33.https://doi.org/10.1007/s00256-020-03465-1
11. Corvino A, Venetucci P, Caruso M, Tarulli FR, Carpiniello M, Pane F, et al. Iliopsoas bursitis: The role of diagnostic imaging in detection, differential diagnosis and treatment. Radiol Case Rep. 2020; 15(11):2149-2152.https://doi.org/10.1016/j.radcr.2020.08.036
12. Wunderbaldinger P, Bremer C, Schellenberger E, Cejna M, Turetschek K, Kainberger F. Imaging features of iliopsoas bursitis. Eur Radiol. 2002; 12(2):409-415.https://doi.org/10.1007/s003300101041
13. Maquirriain J, Ghisi JP, Kokalj AM. Rectus abdominis muscle strains in tennis players. Br J Sports Med. 2007; 41(11):842-848.https://doi.org/10.1136/bjsm.2007.036129
14. Matalon SA, Askari R, Gates JD, Patel K, Sodickson AD, Khurana B. Don't Forget the Abdominal Wall: Imaging Spectrum of Abdominal Wall Injuries after Nonpenetrating Trauma. RadioGraphics. 2017; 37(4):1218-1235.https://doi.org/10.1148/rg.2017160098
15. Kakkar C, Shetty CM, Koteshwara P, Bajpai S. Telltale signs of peripheral neurogenic tumors on magnetic resonance imaging. Indian J Radiol Imaging. 2015; 25(4):453-458.https://doi.org/10.4103/0971-3026.169447
16. Woertler K. Tumors and tumor-like lesions of peripheral nerves. Semin Musculoskelet Radiol. 2010; 14(5):547-558.https://doi.org/10.1055/s-0030-1268073
17. Lucantoni C, Than KD, Wang AC, Valdivia-Valdivia JM, Maher CO, La Marca F, et al. Tarlov cysts: a controversial lesion of the sacral spine. Neurosurg Focus. 2011; 31(6):E14.https://doi.org/10.3171/2011.9.Focus11221
18. Brown E, Matthes JC, Bazan C, 3rd, Jinkins JR. Prevalence of incidental intraspinal lipoma of the lumbosacral spine as determined by MRI. Spine (Phila Pa 1976). 1994; 19(7):833-836.https://doi.org/10.1097/00007632-199404000-00018
19. Warder DE, Oakes WJ. Tethered cord syndrome and the conus in a normal position. Neurosurgery. 1993; 33(3):374-378.https://doi.org/10.1227/00006123-199309000-00004
20. Emery JL, Lendon RG. Lipomas of the cauda equina and other fatty tumours related to neurospinal dysraphism. Dev Med Child Neurol Suppl. 1969; 20:62-70.https://doi.org/10.1111/j.1469-8749.1969.tb09247.x
21. Selden NR. Minimal tethered cord syndrome: what's necessary to justify a new surgical indication? Neurosurgical Focus FOC. 2007; 23(2):1-5.https://doi.org/10.3171/FOC-07/08/E1
22. De Coninck T, Vanhoenacker F, Verstraete K. Imaging Features of Morel-Lavallée Lesions. J Belg Soc Radiol. 2017; 101(Suppl 2):15.https://doi.org/10.5334/jbr-btr.1401
23. Myrick KM, Davis S. Morel-Lavallee injury a case study. Clinical Case Reports. 2018; 6(6):1033-1039.https://doi.org/https://doi.org/10.1002/ccr3.1518
24. Cormio L, Di Fino G, Scavone C, Selvaggio O, Massenio P, Sanguedolce F, et al. Magnetic resonance imaging of penile paraffinoma: case report. BMC Medical Imaging. 2014; 14(1):39.https://doi.org/10.1186/1471-2342-14-39
25. Caskey CI, Berg WA, Hamper UM, Sheth S, Chang BW, Anderson ND. Imaging spectrum of extracapsular silicone: correlation of US, MR imaging, mammographic, and histopathologic findings. Radiographics. 1999; 19 Spec No:S39-51; quiz S261-262.https://doi.org/10.1148/radiographics.19.suppl_1.g99oc11s39

26. Lehnhardt M, Homann HH, Daigeler A, Hauser J, Palka P, Steinau HU. Major and lethal complications of liposuction: a review of 72 cases in Germany between 1998 and 2002. Plast Reconstr Surg. 2008; 121(6):396e-403e.https://doi.org/10.1097/PRS.0b013e318170817a
27. Rozen WM, Ashton MW, Taylor GI. Reviewing the vascular supply of the anterior abdominal wall: redefining anatomy for increasingly refined surgery. Clin Anat. 2008; 21(2):89-98.https://doi.org/10.1002/ca.20585
28. Shridharani SM, Broyles JM, Matarasso A. Liposuction devices: technology update. Med Devices (Auckl). 2014; 7:241-251.https://doi.org/10.2147/mder.S47322
29. Frank SJ, Flusberg M, Friedman S, Swinburne N, Sternschein M, Wolf EL, et al. CT appearance of common cosmetic and reconstructive surgical procedures and their complications. Clin Radiol. 2013; 68(1):e72-78.https://doi.org/10.1016/j.crad.2012.10.001
30. Frank SJ, Flusberg M, Friedman S, Sternschein M, Wolf EL, Stein MW. Aesthetic surgery of the buttocks: imaging appearance. Skeletal Radiol. 2014; 43(2):133-139.https://doi.org/10.1007/s00256-013-1753-x
31. You JS, Chung YE, Baek SE, Chung SP, Kim MJ. Imaging Findings of Liposuction with an Emphasis on Postsurgical Complications. Korean J Radiol. 2015; 16(6):1197-1206.https://doi.org/10.3348/kjr.2015.16.6.1197
32. Hartrampf CR, Scheflan M, Black PW. Breast reconstruction with a transverse abdominal island flap. Plast Reconstr Surg. 1982; 69(2):216-225.https://doi.org/10.1097/00006534-198202000-00006
33. Kanchwala SK, Bucky LP. Optimizing pedicled transverse rectus abdominis muscle flap breast reconstruction. Cancer J. 2008; 14(4):236-240.https://doi.org/10.1097/PPO.0b013e318180bce5
34. Dialani V, Lai KC, Slanetz PJ. MR imaging of the reconstructed breast: What the radiologist needs to know. Insights Imaging. 2012; 3(3):201-213.https://doi.org/10.1007/s13244-012-0150-7
35. Ernst G, Qeadan F, Carlson AP. Subcutaneous bone flap storage after emergency craniectomy: cost-effectiveness and rate of resorption. Journal of Neurosurgery JNS. 2018; 129(6):1604-1610.https://doi.org/10.3171/2017.6.Jns17943
36. Corliss B, Gooldy T, Vaziri S, Kubilis P, Murad G, Fargen K. Complications After In Vivo and Ex Vivo Autologous Bone Flap Storage for Cranioplasty: A Comparative Analysis of the Literature. World Neurosurg. 2016; 96:510-515.https://doi.org/10.1016/j.wneu.2016.09.025
37. Yadla S, Campbell PG, Chitale R, Maltenfort MG, Jabbour P, Sharan AD. Effect of early surgery, material, and method of flap preservation on cranioplasty infections: a systematic review. Neurosurgery. 2011; 68(4):1124-1129; discussion 1130.https://doi.org/10.1227/NEU.0b013e31820a5470
38. Inamasu J, Kuramae T, Nakatsukasa M. Does difference in the storage method of bone flaps after decompressive craniectomy affect the incidence of surgical site infection after cranioplasty? Comparison between subcutaneous pocket and cryopreservation. J Trauma. 2010; 68(1):183-187; discussion 187.https://doi.org/10.1097/TA.0b013e3181c45384
39. Diaz Cascajo C, Borghi S, Weyers W. Panniculitis: definition of terms and diagnostic strategy. Am J Dermatopathol. 2000; 22(6):530-549.https://doi.org/10.1097/00000372-200012000-00009
40. Requena L. Normal subcutaneous fat, necrosis of adipocytes and classification of the panniculitides. Semin Cutan Med Surg. 2007; 26(2):66-70.https://doi.org/10.1016/j.sder.2007.02.001
41. Poh F, Wong SK. Imaging of hidradenitis suppurativa and its complications. Case Rep Radiol. 2014; 2014:294753.https://doi.org/10.1155/2014/294753
42. Napolitano M, Megna M, Timoshchuk EA, Patruno C, Balato N, Fabbrocini G, et al. Hidradenitis suppurativa: from pathogenesis to diagnosis and treatment. Clin Cosmet Investig Dermatol. 2017; 10:105-115.https://doi.org/10.2147/ccid.S111019
43. Margesson LJ, Danby FW. Hidradenitis suppurativa. Best Pract Res Clin Obstet Gynaecol. 2014; 28(7):1013-1027.https://doi.org/10.1016/j.bpobgyn.2014.07.012
44. Kelly AM, Cronin P. MRI features of hidradenitis suppurativa and review of the literature. AJR Am J Roentgenol. 2005; 185(5):1201-1204.https://doi.org/10.2214/ajr.04.1233
45. Monnier L, Dohan A, Amara N, Zagdanski AM, Drame M, Soyer P, et al. Anoperineal disease in Hidradenitis Suppurativa : MR imaging distinction from perianal Crohn's disease. Eur Radiol. 2017; 27(10):4100-4109.https://doi.org/10.1007/s00330-017-4776-1
46. Chan D, Kwon JK, Lagomarsino EM, Veltkamp JG, Yang MS, Pfeifer CM. Canal of Nuck hernias. Acta Radiol Open. 2019; 8(12):2058460119889867.https://doi.org/10.1177/2058460119889867
47. Prodromidou A, Paspala A, Schizas D, Spartalis E, Nastos C, Machairas N. Cyst of the Canal of Nuck in adult females: A case report and systematic review. Biomed Rep. 2020; 12(6):333-338.https://doi.org/10.3892/br.2020.1295
48. Akkoyun I, Kucukosmanoglu I, Yalinkilinc E. Cyst of the canal of nuck in pediatric patients. North American Journal of Medical Sciences. 2013; 5(6):353-356.https://doi.org/10.4103/1947-2714.114166
49. Grosfeld JL. Current concepts in inguinal hernia in infants and children. World J Surg. 1989; 13(5):506-515.https://doi.org/10.1007/bf01658863
50. Cha SH, Romeo MA, Neutze JA. Visceral manifestations of Klippel-Trénaunay syndrome. Radiographics. 2005; 25(6):1694-1697.https://doi.org/10.1148/rg.256055042
51. Guillin R, Moser T, Koob M, Khoury V, Chapuis M, Ropars M, et al. Subperiosteal hematoma of the iliac bone: imaging features of acute and chronic stages with emphasis on pathophysiology. Skeletal Radiol. 2012; 41(6):667-675.https://doi.org/10.1007/s00256-011-1267-3
52. Jee WH, Choi KH, Choe BY, Park JM, Shinn KS. Fibrous dysplasia: MR imaging characteristics with radiopathologic correlation. AJR Am J Roentgenol. 1996; 167(6):1523-1527.https://doi.org/10.2214/ajr.167.6.8956590
53. Lee JS, FitzGibbon EJ, Chen YR, Kim HJ, Lustig LR, Akintoye SO, et al. Clinical guidelines for the management of craniofacial fibrous dysplasia. Orphanet J Rare Dis. 2012; 7 Suppl 1(Suppl 1):S2.https://doi.org/10.1186/1750-1172-7-s1-s2